ESAIM: M2AN 54 (2020) 2045–2067
https://doi.org/10.1051/m2an/2020035

ESAIM: Mathematical Modelling and Numerical Analysis
www.esaim-m2an.org

A PARAMETER-ROBUST ITERATIVE METHOD FOR STOKES–DARCY PROBLEMS RETAINING LOCAL MASS CONSERVATION

Wietse M. Boon[1,2,*]

Abstract. We consider a coupled model of free-flow and porous medium flow, governed by stationary Stokes and Darcy flow, respectively. The coupling between the two systems is enforced by introducing a single variable representing the normal flux across the interface. The problem is reduced to a system concerning only the interface flux variable, which is shown to be well-posed in appropriately weighted norms. An iterative solution scheme is then proposed to solve the reduced problem such that mass is conserved at each iteration. By introducing a preconditioner based on the weighted norms from the analysis, the performance of the iterative scheme is shown to be robust with respect to material and discretization parameters. By construction, the scheme is applicable to a wide range of locally conservative discretization schemes and we consider explicit examples in the framework of Mixed Finite Element methods. Finally, the theoretical results are confirmed with the use of numerical experiments.

Mathematics Subject Classification. 65N12, 65N55, 76D07, 76S05.

Received July 22, 2019. Accepted May 6, 2020.

1. Introduction

The coupled interaction between free flow and porous medium flow forms an active area of research due to their appearance in a wide variety of applications. Examples include biomedical applications such as blood filtration, engineering situations such as air filters and PEM fuel cells, as well as environmental considerations such as the drying of soils. In all mentioned applications, it is essential to properly capture the mutual interaction between a free, possibly turbulent, flow and the creeping flow inside the porous medium.

We consider the simplified setting in which the free-flow regime is described by Stokes flow and we let Darcy's law govern the porous medium flow. Moreover, we only consider the case of stationary, single-phase flow and assume a sharp interface between the two flow regimes. These considerations are simplifications of a more general framework of models coupling free flow with porous medium flow. Such models have been the topic of a variety of scientific work in recent years, with focuses including mathematical analysis, discretization methods, and iterative solution techniques. Different formulations of the Stokes–Darcy problem have been analyzed in [9, 19, 23]. Examples in the context of discretization methods include the use of Finite Volume

Keywords and phrases. Coupled porous media and fluid flow, Mixed Finite Element method, mortar method, robust preconditioner.

[1] University of Stuttgart, Department of Hydromechanics and Modelling of Hydrosystems, Pfaffenwaldring 61, Stuttgart 70569, Germany.

[2] KTH Royal Institute of Technology, Department of Mathematics, Lindstedtsvägen 25, Stockholm 114 28, Sweden.

*Corresponding author: wietse@kth.se

methods [15, 20, 27, 28, 34, 36] and (Mixed) Finite Element methods, both in a coupled [12, 18, 23, 32] and in a unified [2, 21] setting. Moreover, iterative methods for this problem are considered in *e.g.* [8, 10, 11, 13, 16, 17]. We refer the reader to the works [9, 12, 33] and references therein for more comprehensive overviews on the results concerning the Stokes–Darcy model.

In order to distinguish this work from existing results, we formulate the following objective:
The goal of this work is to create an iterative numerical method that solves the stationary, Stokes–Darcy problem with the following three properties:

(1) The solution retains *local mass conservation*, after each iteration. Since mass balance is a physical conservation law, we emphasize its importance over all other constitutive relationships in the model. Hence, the first aim is to produce a solution that respects local mass conservation and use iterations to improve the accuracy of the solution with respect to the remaining equations. Importantly, we aim to obtain a conservative flow field in the case that the iterative scheme is terminated before reaching convergence.

    We present two main ideas to achieve this. First, we limit ourselves to discretization methods capable of ensuring local mass conservation within each flow regime. Secondly, we ensure that no mass is lost across the Stokes–Darcy interface by introducing a single variable describing this interfacial flux. Our contribution in this context is to pose and analyze the Stokes–Darcy problem using function spaces that ensure normal flux continuity (Sect. 2.1), both in the continuous (Sect. 3) and discretized (Sect. 5) settings. Our approach is closely related to the "global" approach suggested in Remark 2.3.2 of [9] which we further develop in a functional setting. We moreover note that our construction is, in a sense, dual to the more conventional approach in which a mortar variable representing the interface pressure is introduced, see *e.g.* [18, 23].

(2) The performance of the iterative solution scheme is *robust with respect to physical and mesh parameters*. In this respect, the first aim is to obtain sufficient accuracy of the solution within a given number of iterations that is robust with respect to given material parameters such as the permeability of the porous medium and the viscosity of the fluid. This will allow the scheme to handle wide ranges of material parameters that arise either from the physical problem or due to the chosen non-dimensionalization.

    Robustness with respect to mesh size is advantageous from a computational perspective. If the scheme reaches sufficient accuracy within a number of iterations on a coarse grid, then this robustness provides a prediction on the necessary computational time on refined grids. We note that the analysis in this work is restricted to shape-regular meshes, hence the typical mesh size h becomes the only relevant mesh parameter. To attain this goal, we pay special attention to the influence of the material and mesh parameters in the *a priori* analysis of the problem. We derive stability bounds of the solution in terms of functional norms weighted with the material parameters. One of the main contributions is thus the derivation of a properly weighted norm for the normal flux on the Stokes–Darcy interface, presented in equation (4.5). In turn, this norm is used to construct an optimal preconditioner *a priori*.

(3) The method is easily extendable to a *wide range of discretization methods* for the Stokes and Darcy subproblems. Aside from compliance with aim (1), we impose as few restrictions as possible on the underlying choice of discretization methods, thus allowing the presented iterative scheme to be highly adaptable. Moreover, the scheme is able to benefit from existing numerical implementations that are tailored to solving the Stokes and Darcy subproblems efficiently. This work employs a conforming Mixed Finite Element method, keeping in mind that extensions can readily be made to other locally conservative methods such as *e.g.* Finite Volume Methods or Discontinuous Galerkin methods.

    In order to achieve this third goal, we first derive the properties of the problem in the continuous setting and apply the discretization afterward. The key strategy here is to reformulate the problem into a Steklov–Poincaré system concerning only the normal flux across the interface, similar to the strategy presented in Section 2.5 of [9]. We then propose a preconditioner for this problem that is independent of the chosen discretization methods for the subproblems.

Our formulation and analysis of the Stokes–Darcy problem therefore has three distinguishing properties. Most importantly, we consider a mixed formulation of the coupled problem using a function space that strongly

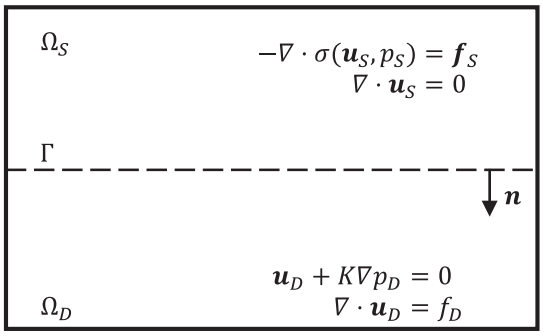

FIGURE 1. Decomposition of the domain into Ω_S and Ω_D.

imposes normal flux continuity at the interface. In contrast, existing approaches often use a primal formulation for the Darcy subproblem [9] or enforce flux continuity using Lagrange multipliers [23]. In the context of Mixed Finite Element methods, this directly leads to different choices of discrete spaces. Secondly, our analysis employs weighted norms and we derive an estimate for the interface flux that has, to our knowledge, not been exploited in existing literature. Third, we propose a preconditioner in Section 6.2 that is entirely local to the interface and does not require additional subproblem solves, in contrast to more conventional approaches such as the Neumann–Neumann method presented in Section 7.2. The construction of this preconditioner does, however, require solving a generalized eigenvalue problem, which is done in the *a priori*, or "off-line", stage. As an additional feature, our set-up does not require choosing any acceleration parameters.

The article is structured as follows. Section 2 introduces the coupled Stokes–Darcy model and its variational formulation as well as the notational conventions used throughout this work. Well-posedness of the model is shown in Section 3 with the use of weighted norms. Section 4 shows the reduction to an interface problem concerning only the normal flux defined there. A conforming discretization is proposed in Section 5 with the use of the Mixed Finite Element method. Using the ingredients of these sections, Section 6 describes the proposed iterative scheme and the optimal preconditioner it relies on. The theoretical results are confirmed numerically in Section 7. Finally, Section 8 contains concluding remarks.

2. The coupled Stokes–Darcy model

Consider an open, bounded domain $\Omega \subset \mathbb{R}^n$, $n \in \{2, 3\}$, decomposed into two disjoint, Lipschitz subdomains Ω_S and Ω_D. Here, and throughout this work, the subscript S or D is used on subdomains and variables to denote its association to the Stokes or Darcy subproblem, respectively. Let the interface be denoted by $\Gamma := \partial\Omega_S \cap \partial\Omega_D$ and let $\boldsymbol{n}$ denote the unit vector normal to Γ oriented outward with respect to Ω_S. An illustration of these definitions is given in Figure 1.

We introduce the model problem following the description of [23]. The main variables are given by the velocity $\boldsymbol{u}$ and pressure p. A subscript denotes the restriction of a variable to the corresponding subdomain. The model is formed by considering Stokes flow for $(\boldsymbol{u}_S, p_S)$ in Ω_S, Darcy flow for $(\boldsymbol{u}_D, p_D)$ in Ω_D, and mass conservation laws for $\boldsymbol{u}$ in both subdomains:

$$-\nabla \cdot \sigma(\boldsymbol{u}_S, p_S) = \boldsymbol{f}_S, \qquad \nabla \cdot \boldsymbol{u}_S = 0, \qquad \text{in } \Omega_S, \tag{2.1a}$$

$$\boldsymbol{u}_D + K\nabla p_D = 0, \qquad \nabla \cdot \boldsymbol{u}_D = f_D, \qquad \text{in } \Omega_D. \tag{2.1b}$$

In this setting, K is the hydraulic conductivity of the porous medium. For simplicity, we assume that K is homogeneous and isotropic and thus given by a positive scalar. On the right-hand side, $\boldsymbol{f}_S$ represents a body force and f_D corresponds to a mass source. In the governing equations for Stokes flow, let the strain ε and stress

σ be given by

$$\varepsilon(\boldsymbol{u}_S) := \frac{1}{2}\left(\nabla \boldsymbol{u}_S + (\nabla \boldsymbol{u}_S)^T\right), \qquad \sigma(\boldsymbol{u}_S, p_S) := \mu\varepsilon(\boldsymbol{u}_S) - p_S I.$$

The parameter $\mu > 0$ is the viscosity.

Next, we introduce two coupling conditions on the interface Γ that describe mass conservation and the balance of forces, respectively:

$$\boldsymbol{n} \cdot \boldsymbol{u}_S = \boldsymbol{n} \cdot \boldsymbol{u}_D, \qquad \text{on } \Gamma, \tag{2.1c}$$

$$\boldsymbol{n} \cdot \sigma(\boldsymbol{u}_S, p_S) \cdot \boldsymbol{n} = -p_D, \qquad \text{on } \Gamma. \tag{2.1d}$$

As remarked in the introduction, we keep a particular focus on conservation of mass. To ensure that no mass is lost across the interface, we will prioritize condition (2.1c) at a later stage.

To close the model, we consider the following boundary conditions. First, for the Stokes subproblem, we impose the Beavers–Joseph–Saffman condition on the interface Γ, given by

$$\boldsymbol{n} \cdot \sigma(\boldsymbol{u}_S, p_S) \cdot \boldsymbol{\tau} = -\beta \boldsymbol{\tau} \cdot \boldsymbol{u}_S, \qquad \text{on } \Gamma. \tag{2.1e}$$

Here, we define $\beta := \alpha \frac{\mu}{\sqrt{\boldsymbol{\tau}\cdot\kappa\cdot\boldsymbol{\tau}}}$ with $\kappa := \mu K$ the permeability and α a proportionality constant to be determined experimentally. Moreover, the unit vector $\boldsymbol{\tau}$ is obtained from the tangent bundle of Γ. Thus, for $n = 2$, equation (2.1e) corresponds to a single condition on the one-dimensional interface Γ whereas for $n = 3$, it describes two separate coupling conditions.

The boundary of Ω is decomposed in the disjoint unions $\partial\Omega_S \setminus \Gamma = \partial_u\Omega_S \cup \partial_\sigma\Omega_S$ and $\partial\Omega_D \setminus \Gamma = \partial_u\Omega_D \cup \partial_p\Omega_D$. The subscript denotes the type of boundary condition imposed on that portion of the boundary. Specifically, we set

$$\boldsymbol{u}_S = 0, \quad \text{on } \partial_u\Omega_S, \qquad \boldsymbol{n} \cdot \boldsymbol{u}_D = 0, \quad \text{on } \partial_u\Omega_D. \tag{2.1f}$$

$$\boldsymbol{n} \cdot \sigma(\boldsymbol{u}_S, p_S) = 0, \quad \text{on } \partial_\sigma\Omega_S, \qquad p_D = g_p, \quad \text{on } \partial_p\Omega_D, \tag{2.1g}$$

with g_p a given pressure distribution.

In the following, we assume that the interface Γ touches the portion of the boundary $\partial\Omega_S$ where homogeneous flux conditions are imposed, *i.e.* $\partial\Gamma \subseteq \overline{\partial_u\Omega_S}$. We note that this assumption excludes the case in which Ω_D is completely surrounded by Ω_S. Moreover, we assume that $|\partial_\sigma\Omega_S \cup \partial_p\Omega_D| > 0$ to ensure unique solvability of the coupled problem and we focus on the case in which $|\partial_\sigma\Omega_S| > 0$.

2.1. Functional setting

In this section, we introduce the function spaces in which we search for a weak solution of problem (2.1). We start by considering the space for the velocity variable $\boldsymbol{u}$. With the aim of deriving mixed formulations for both subproblems, we introduce the following spaces:

$$\boldsymbol{V}_S := \left\{ \boldsymbol{v}_S \in \left(H^1(\Omega_S)\right)^n : \ \boldsymbol{v}_S|_{\partial_u\Omega_S} = 0 \right\}, \tag{2.2a}$$

$$\boldsymbol{V}_D := \left\{ \boldsymbol{v}_D \in H(\mathrm{div}, \Omega_D) : \ \boldsymbol{n} \cdot \boldsymbol{v}_D|_{\partial_u\Omega_D} = 0 \right\}. \tag{2.2b}$$

Note that these spaces incorporate the boundary conditions (2.1f) on $\partial_u\Omega$ which become essential boundary conditions in our mixed formulation. Similarly, the normal flux continuity across Γ (2.1c) needs to be incorporated as an essential boundary condition. For that, we introduce a single function $\phi \in \Lambda$, defined on Γ to represent the normal flux across the interface. The next step is then to define the following three function spaces:

$$\boldsymbol{V}_S^0 := \left\{ \boldsymbol{v}_S \in \boldsymbol{V}_S : \ \boldsymbol{n} \cdot \boldsymbol{v}_S|_\Gamma = 0 \right\}, \tag{2.3a}$$

$$\Lambda := H_{00}^{1/2}(\Gamma), \tag{2.3b}$$

$$\boldsymbol{V}_D^0 := \left\{ \boldsymbol{v}_D \in \boldsymbol{V}_D : \ \boldsymbol{n} \cdot \boldsymbol{v}_D|_\Gamma = 0 \right\}. \tag{2.3c}$$

We note that Λ is the normal trace space of $\boldsymbol{V}_S$ on Γ. From the previous section, we recall that Γ touches the boundary $\partial\Omega$ where zero velocity conditions are imposed for the Stokes problem. The trace space is therefore characterized as the fractional Sobolev space $H_{00}^{1/2}(\Gamma)$, containing distributions that can be continuously extended by zero on $\partial\Omega$. We refer the reader to [24] for more details on this type of trace spaces. For the purpose of our analysis, we note that the inclusion $H_0^1(\Gamma) \subset \Lambda \subset L^2(\Gamma)$ holds and we let $H^{-\frac{1}{2}}(\Gamma)$ denote the dual of Λ.

For the incorporation of the interface condition (2.1c) in our weak formulation, we introduce continuous operators that extend a given flux distribution on the interface to the two subdomains. The extension operators $\mathcal{R}_S : \Lambda \to \boldsymbol{V}_S$ and $\mathcal{R}_D : \Lambda \to \boldsymbol{V}_D$ are chosen such that

$$(\boldsymbol{n} \cdot \mathcal{R}_S\varphi)|_\Gamma = (\boldsymbol{n} \cdot \mathcal{R}_D\varphi)|_\Gamma = \varphi. \tag{2.4}$$

We use $\|\cdot\|_{s,\Omega}$ as short-hand notation for the norm on $H^s(\Omega)$. With this notation, the continuity of $\mathcal{R}_i$ implies that the following inequalities hold

$$\|\mathcal{R}_S\varphi\|_{1,\Omega_S} \lesssim \|\varphi\|_{\frac{1}{2},\Gamma}, \qquad \|\mathcal{R}_D\varphi\|_{0,\Omega_D} + \|\nabla \cdot \mathcal{R}_D\varphi\|_{0,\Omega_D} \lesssim \|\varphi\|_{-\frac{1}{2},\Gamma}. \tag{2.5}$$

Examples of continuous extension operators can be found in Section 4.1.2 of [30]. The notation $A \lesssim B$ implies that a constant $c > 0$ exists, independent of material parameters and the mesh size h such that $A \leq cB$. The relationship $\gtrsim$ is defined analogously.

These definitions allow us to create a function space $\boldsymbol{V}$ containing velocities with normal trace continuity on Γ. Let this function space be defined as

$$\boldsymbol{V} := \left\{ \boldsymbol{v} \in \left(L^2(\Omega)\right)^n : \ \exists \left(\boldsymbol{v}_S^0, \varphi, \boldsymbol{v}_D^0\right) \in \boldsymbol{V}_S^0 \times \Lambda \times \boldsymbol{V}_D^0 \text{ such that } \boldsymbol{v}|_{\Omega_i} = \boldsymbol{v}_i^0 + \mathcal{R}_i\varphi, \text{ for } i \in \{S, D\} \right\}. \tag{2.6}$$

Second, the function space for the pressure variable is given by $W := L^2(\Omega)$ and we define $W_S := L^2(\Omega_S)$ and $W_D := L^2(\Omega_D)$.

As before, we use the subscript $i \in \{S, D\}$ to denote the restriction to a subdomain Ω_i. Thus, for $(\boldsymbol{v}, w) \in \boldsymbol{V} \times W$, we have

$$\boldsymbol{v}_i := \boldsymbol{v}|_{\Omega_i} \in \boldsymbol{V}_i, \qquad w_i := w|_{\Omega_i} \in W_i, \qquad i \in \{S, D\}. \tag{2.7}$$

Despite the fact that each function in $\boldsymbol{V}$ can be decomposed into components in $\boldsymbol{V}_S$ and $\boldsymbol{V}_D$, we emphasize that $\boldsymbol{V}$ is a strict subspace of $\boldsymbol{V}_S \times \boldsymbol{V}_D$ due to the continuity of normal traces on Γ.

A key concept in our functional setting is to consider a decomposition of $\boldsymbol{V}$ comprising of a function with zero normal trace on Γ and an extension of the normal flux distribution. For that purpose, let $\boldsymbol{V}^0$ be the subspace of $\boldsymbol{V}$ consisting of functions with zero normal trace over Γ:

$$\boldsymbol{V}^0 := \left\{ \boldsymbol{v}^0 \in \boldsymbol{V} : \ \exists \left(\boldsymbol{v}_S^0, \boldsymbol{v}_D^0\right) \in \boldsymbol{V}_S^0 \times \boldsymbol{V}_D^0 \text{ such that } \boldsymbol{v}^0|_{\Omega_i} = \boldsymbol{v}_i^0, \text{ for } i \in \{S, D\} \right\}. \tag{2.8}$$

Secondly, we define the composite extension operator $\mathcal{R} : \Lambda \to V$ such that $\mathcal{R}\varphi|_{\Omega_i} = \mathcal{R}_i\varphi$ for $i \in \{S, D\}$. Combined with the subspace $\boldsymbol{V}^0$, we obtain the decomposition

$$\boldsymbol{V} = \boldsymbol{V}^0 \oplus \mathcal{R}\Lambda. \tag{2.9}$$

It is important to emphasize that the function space $\boldsymbol{V}$ is independent of the choice of extension operators. On the other hand, each choice of $\mathcal{R}$ leads to a specific decomposition of the form (2.9).

2.2. Variational formulation

With the function spaces defined, we continue by deriving the variational formulation of (2.1). The first step is to consider the Stokes and Darcy flow equations. We test these with $\boldsymbol{v} \in \boldsymbol{V}$ and integrate over the

corresponding subdomain. Using $(\cdot,\cdot)_\Omega$ to denote the L^2 inner product on Ω, we apply integration by parts and use the boundary conditions to derive

$$\begin{aligned} -(\nabla\cdot\sigma(\boldsymbol{u}_S,p_S),\boldsymbol{v}_S)_{\Omega_S} &= \\ (\sigma(\boldsymbol{u}_S,p_S),\nabla\boldsymbol{v}_S)_{\Omega_S} - (\boldsymbol{n}\cdot\sigma(\boldsymbol{u}_S,p_S),\boldsymbol{v}_S)_\Gamma &= \\ (\mu\varepsilon(\boldsymbol{u}_S),\varepsilon(\boldsymbol{v}_S))_{\Omega_S} - (p_S I,\nabla\boldsymbol{v}_S)_{\Omega_S} + (\beta\boldsymbol{\tau}\cdot\boldsymbol{u}_S,\boldsymbol{\tau}\cdot\boldsymbol{v}_S)_\Gamma + (p_D,\boldsymbol{n}\cdot\boldsymbol{v}_S)_\Gamma &= (\boldsymbol{f}_S,\boldsymbol{v}_S)_\Omega. \end{aligned}$$

On the other hand, we test Darcy's law in the porous medium Ω_D and use similar steps to obtain

$$\left(K^{-1}\boldsymbol{u}_D,\boldsymbol{v}_D\right)_{\Omega_D} - (p_D,\nabla\cdot\boldsymbol{v}_D)_{\Omega_D} - (p_D,\boldsymbol{n}\cdot\boldsymbol{v}_D)_\Gamma - (g_p,\boldsymbol{n}\cdot\boldsymbol{v}_D)_{\partial_p\Omega_D} = 0.$$

The normal trace continuity imposed in the space $\boldsymbol{V}$ gives us $(p_D,\boldsymbol{n}\cdot\boldsymbol{v}_S)_\Gamma - (p_D,\boldsymbol{n}\cdot\boldsymbol{v}_D)_\Gamma = 0$.

In turn, after supplementing the system with the equations for mass conservation, we arrive at the following variational formulation.

Find the pair $(\boldsymbol{u},p)\in\boldsymbol{V}\times W$ that satisfies

$$\begin{aligned} &(\mu\varepsilon(\boldsymbol{u}_S),\varepsilon(\boldsymbol{v}_S))_{\Omega_S} + (\beta\boldsymbol{\tau}\cdot\boldsymbol{u}_S,\boldsymbol{\tau}\cdot\boldsymbol{v}_S)_\Gamma + \left(K^{-1}\boldsymbol{u}_D,\boldsymbol{v}_D\right)_{\Omega_D} \\ &\quad -(p_S,\nabla\cdot\boldsymbol{v}_S)_{\Omega_S} - (p_D,\nabla\cdot\boldsymbol{v}_D)_{\Omega_D} = (\boldsymbol{f}_S,\boldsymbol{v}_S)_{\Omega_S} + (g_p,\boldsymbol{n}\cdot\boldsymbol{v}_D)_{\partial_p\Omega_D}, \qquad \forall\boldsymbol{v}\in\boldsymbol{V}, \qquad (2.10a) \\ &\quad (\nabla\cdot\boldsymbol{u}_S,w_S)_{\Omega_S} + (\nabla\cdot\boldsymbol{u}_D,w_D)_{\Omega_D} = (f_D,w_D)_{\Omega_D}, \qquad \forall w\in W. \qquad (2.10b) \end{aligned}$$

We note that this system has a characteristic saddle-point structure, allowing us to rewrite the problem as:

Find the pair $(\boldsymbol{u},p)\in\boldsymbol{V}\times W$ that satisfies

$$\begin{aligned} a(\boldsymbol{u},\boldsymbol{v}) + b(\boldsymbol{v},p) &= f_u(\boldsymbol{v}), \qquad \forall\boldsymbol{v}\in\boldsymbol{V}, \qquad (2.11a) \\ b(\boldsymbol{u},w) &= f_p(w), \qquad \forall w\in W. \qquad (2.11b) \end{aligned}$$

The bilinear forms $a:\boldsymbol{V}\times\boldsymbol{V}\to\mathbb{R}$ and $b:\boldsymbol{V}\times W\to\mathbb{R}$, and the functionals $f_u:\boldsymbol{V}\to\mathbb{R}$ and $f_p:W\to\mathbb{R}$ are given by

$$\begin{aligned} a(\boldsymbol{u},\boldsymbol{v}) &:= (\mu\varepsilon(\boldsymbol{u}_S),\varepsilon(\boldsymbol{v}_S))_{\Omega_S} + (\beta\boldsymbol{\tau}\cdot\boldsymbol{u}_S,\boldsymbol{\tau}\cdot\boldsymbol{v}_S)_\Gamma + \left(K^{-1}\boldsymbol{u}_D,\boldsymbol{v}_D\right)_{\Omega_D}, \qquad (2.12a) \\ b(\boldsymbol{u},w) &:= -(\nabla\cdot\boldsymbol{u}_S,w_S)_{\Omega_S} - (\nabla\cdot\boldsymbol{u}_D,w_D)_{\Omega_D}, \qquad (2.12b) \\ f_u(\boldsymbol{v}) &:= (\boldsymbol{f}_S,\boldsymbol{v}_S)_{\Omega_S} + (g_p,\boldsymbol{n}\cdot\boldsymbol{v}_D)_{\partial_p\Omega_D}, \qquad (2.12c) \\ f_p(w) &:= -(f_D,w_D)_{\Omega_D}. \qquad (2.12d) \end{aligned}$$

3. Well-posedness analysis

In this section, we analyze problem (2.11) with the use of weighted norms. The main goal is to show that a unique solution exists that is bounded in norms that depend on the material parameters. Consequently, this result allows us to construct an iterative method that is robust with respect to material parameters. We start by deriving the appropriate norms, for which we first make two assumptions on the material parameters.

First, the constant β in the Beavers–Joseph–Saffman condition (2.1e) is assumed to be bounded as

$$\beta = \alpha\frac{\mu}{\sqrt{\boldsymbol{\tau}\cdot\kappa\cdot\boldsymbol{\tau}}} \lesssim \mu. \qquad (3.1a)$$

In the special case of $\alpha = 0$, this condition is trivially satisfied.

Second, we assume that the permeability $\kappa := \mu K$ is bounded from above in the sense that

$$\mu K \lesssim 1. \qquad (3.1b)$$

We are now ready to define the weighted norms for $\boldsymbol{v} \in \boldsymbol{V}$ and $w \in W$, respectively, given by

$$\|\boldsymbol{v}\|_V^2 := \|\mu^{\frac{1}{2}} \boldsymbol{v}_S\|_{1,\Omega_S}^2 + \|K^{-\frac{1}{2}} \boldsymbol{v}_D\|_{0,\Omega_D}^2 + \|K^{-\frac{1}{2}} \nabla \cdot \boldsymbol{v}_D\|_{0,\Omega_D}^2 \tag{3.2a}$$

$$\|w\|_W^2 := \|\mu^{-\frac{1}{2}} w_S\|_{0,\Omega_S}^2 + \|K^{\frac{1}{2}} w_D\|_{0,\Omega_D}^2. \tag{3.2b}$$

The next step is to analyze the problem using these norms. For that purpose, we recall the identification of (2.11) as a saddle-point problem. Using saddle-point theory [5], well-posedness is shown by proving the four sufficient conditions presented in the following lemma.

Lemma 3.1. *The bilinear forms defined in* (2.12) *satisfy the following inequalities:*

$$\text{For } \boldsymbol{u}, \boldsymbol{v} \in \boldsymbol{V}: \qquad a(\boldsymbol{u}, \boldsymbol{v}) \lesssim \|\boldsymbol{u}\|_V \|\boldsymbol{v}\|_V. \tag{3.3a}$$

$$\text{For } (\boldsymbol{v}, w) \in \boldsymbol{V} \times W: \qquad b(\boldsymbol{v}, w) \lesssim \|\boldsymbol{v}\|_V \|w\|_W. \tag{3.3b}$$

$$\text{For } \boldsymbol{v} \in \boldsymbol{V} \text{ with } b(\boldsymbol{v}, w) = 0 \ \forall w \in W: \qquad a(\boldsymbol{v}, \boldsymbol{v}) \gtrsim \|\boldsymbol{v}\|_V^2. \tag{3.3c}$$

$$\text{For } w \in W, \ \exists \boldsymbol{v} \in \boldsymbol{V} \text{ with } \boldsymbol{v} \neq 0, \text{ such that:} \qquad b(\boldsymbol{v}, w) \gtrsim \|\boldsymbol{v}\|_V \|w\|_W. \tag{3.3d}$$

Proof. Using the Cauchy–Schwarz inequality, the assumptions (3.1), and a trace inequality for H^1, we obtain the continuity bounds (3.3a) and (3.3b):

$$\begin{aligned} a(\boldsymbol{u}, \boldsymbol{v}) &\lesssim \|\mu^{\frac{1}{2}} \boldsymbol{u}_S\|_{1,\Omega_S} \|\mu^{\frac{1}{2}} \boldsymbol{v}_S\|_{1,\Omega_S} + \|\beta^{\frac{1}{2}} \boldsymbol{\tau} \cdot \boldsymbol{u}_S\|_{0,\Gamma} \|\beta^{\frac{1}{2}} \boldsymbol{\tau} \cdot \boldsymbol{v}_S\|_{0,\Gamma} + \|K^{-\frac{1}{2}} \boldsymbol{u}_D\|_{0,\Omega_D} \|K^{-\frac{1}{2}} \boldsymbol{v}_D\|_{0,\Omega_D} \\ &\lesssim \|\boldsymbol{u}\|_V \|\boldsymbol{v}\|_V, \end{aligned} \tag{3.4a}$$

$$\begin{aligned} b(\boldsymbol{v}, w) &\lesssim \|\mu^{\frac{1}{2}} \boldsymbol{v}_S\|_{1,\Omega_S} \|\mu^{-\frac{1}{2}} w_S\|_{0,\Omega_S} + \|K^{-\frac{1}{2}} \nabla \cdot \boldsymbol{v}_D\|_{0,\Omega_D} \|K^{\frac{1}{2}} w_D\|_{0,\Omega_D} \\ &\lesssim \|\boldsymbol{v}\|_V \|w\|_W. \end{aligned} \tag{3.4b}$$

For the proof of inequality (3.3c), we first note that if $b(\boldsymbol{v}, w) = 0$ for all $w \in W$, then $\nabla \cdot \boldsymbol{v}_D = 0$. Combining this observation with Korn's inequality gives us:

$$\begin{aligned} a(\boldsymbol{v}, \boldsymbol{v}) &\gtrsim \|\mu^{\frac{1}{2}} \boldsymbol{v}_S\|_{1,\Omega_S}^2 + \|\beta^{\frac{1}{2}} \boldsymbol{\tau} \cdot \boldsymbol{v}_S\|_{0,\Gamma}^2 + \|K^{-\frac{1}{2}} \boldsymbol{v}_D\|_{0,\Omega_D}^2 \\ &\geq \|\mu^{\frac{1}{2}} \boldsymbol{v}_S\|_{1,\Omega_S}^2 + \|K^{-\frac{1}{2}} \nabla \cdot \boldsymbol{v}_D\|_{0,\Omega_D}^2 + \|K^{-\frac{1}{2}} \boldsymbol{v}_D\|_{0,\Omega_D}^2 = \|\boldsymbol{v}\|_V^2. \end{aligned} \tag{3.5}$$

Inequality (3.3d) is the inf-sup condition relevant for this formulation. For a given $w = (w_S, w_D) \in W$, let us construct $\boldsymbol{v} = (\boldsymbol{v}_S^0, \phi, \boldsymbol{v}_D^0) \in \boldsymbol{V}$ in the following manner. First, let the interface function $\phi \in H_0^1(\Gamma)$ solve the following, constrained minimization problem:

$$\min_{\varphi \in H_0^1(\Gamma)} \tfrac{1}{2} \|\varphi\|_{1,\Gamma}^2, \text{ subject to } (\varphi, 1)_\Gamma = (K w_D, 1)_{\Omega_D}. \tag{3.6}$$

The solution ϕ then satisfies the two key properties:

$$\|\phi\|_{1,\Gamma} \lesssim \|K w_D\|_{0,\Omega_D}, \tag{3.7a}$$

$$(\nabla \cdot \mathcal{R}_D \phi, 1)_{\Omega_D} = (-\boldsymbol{n} \cdot \mathcal{R}_D \phi, 1)_\Gamma = (-\phi, 1)_\Gamma = -(K w_D, 1)_{\Omega_D}. \tag{3.7b}$$

Bound (3.7a) can be deduced by constructing a function $\psi \in H_0^1(\Gamma)$ that satisfies the constraint in (3.6) and is bounded in the sense of (3.7a). It then follows that the minimizer ϕ satisfies (3.7a) as well.

Next, we construct $\boldsymbol{v}_i^0 \in \boldsymbol{V}_i^0$ for $i \in \{S, D\}$. For that, we first introduce $p_S \in H^2(\Omega_S)$ as the solution to the following auxiliary problem

$$-\nabla \cdot \nabla p_S = \mu^{-1} w_S + \nabla \cdot \mathcal{R}_S \phi, \tag{3.8a}$$

$$p_S|_{\partial_\sigma \Omega_S} = 0, \tag{3.8b}$$

$$(\boldsymbol{n} \cdot \nabla p_S)|_{\partial \Omega_S \setminus \partial_\sigma \Omega_S} = 0. \tag{3.8c}$$

Similarly, we define $p_D \in H^2(\Omega_D)$ such that

$$-\nabla \cdot \nabla p_D = K w_D + \nabla \cdot \mathcal{R}_D \phi, \tag{3.9a}$$
$$(\boldsymbol{n} \cdot \nabla p_D)|_{\partial\Omega_D} = 0. \tag{3.9b}$$

We note that (3.9) is a Neumann problem. We therefore verify the compatibility of the right hand side by using (3.7b) in the following derivation:

$$(K w_D + \nabla \cdot \mathcal{R}_D \phi, 1)_{\Omega_D} = (K w_D - K w_D, 1)_{\Omega_D} = 0.$$

Let $\boldsymbol{v}_S^0 := \nabla p_S$ and $\boldsymbol{v}_D^0 := \nabla p_D$. From the elliptic regularity of the auxiliary problems, see *e.g.* [14], we obtain the bounds

$$\|\boldsymbol{v}_S^0\|_{1,\Omega_S} \lesssim \|\mu^{-1} w_S\|_{0,\Omega_S} + \|\nabla \cdot \mathcal{R}_S \phi\|_{0,\Omega_S}, \tag{3.10a}$$
$$\|\boldsymbol{v}_D^0\|_{1,\Omega_D} \lesssim \|K w_D\|_{0,\Omega_D} + \|\nabla \cdot \mathcal{R}_D \phi\|_{0,\Omega_D}. \tag{3.10b}$$

Next, we set $\boldsymbol{v}_S := \boldsymbol{v}_S^0 + \mathcal{R}_S \phi$ and $\boldsymbol{v}_D := \boldsymbol{v}_D^0 + \mathcal{R}_D \phi$. Combining the bounds on $\boldsymbol{v}_S^0$ and ϕ with the continuity of the extension operators from (2.5) and the material parameter bounds (3.1), we derive

$$\begin{aligned}
\|\mu^{\frac{1}{2}} \boldsymbol{v}_S\|_{1,\Omega_S} &\leq \|\mu^{\frac{1}{2}} \boldsymbol{v}_S^0\|_{1,\Omega_S} + \|\mu^{\frac{1}{2}} \mathcal{R}_S \phi\|_{1,\Omega_S} \\
&\lesssim \|\mu^{-\frac{1}{2}} w_S\|_{0,\Omega_S} + \|\mu^{\frac{1}{2}} \nabla \cdot \mathcal{R}_S \phi\|_{0,\Omega_S} + \|\mu^{\frac{1}{2}} \mathcal{R}_S \phi\|_{1,\Omega_S} \\
&\lesssim \|\mu^{-\frac{1}{2}} w_S\|_{0,\Omega_S} + \|\mu^{\frac{1}{2}} \phi\|_{\frac{1}{2},\Gamma} \\
&\lesssim \|\mu^{-\frac{1}{2}} w_S\|_{0,\Omega_S} + \|\mu^{\frac{1}{2}} K w_D\|_{0,\Omega_D} \\
&\lesssim \|\mu^{-\frac{1}{2}} w_S\|_{0,\Omega_S} + \|K^{\frac{1}{2}} w_D\|_{0,\Omega_D}.
\end{aligned} \tag{3.11a}$$

Similarly, $\boldsymbol{v}_D$ is bounded in the following sense:

$$\begin{aligned}
\|K^{-\frac{1}{2}} \boldsymbol{v}_D\|_{0,\Omega_D} + \|K^{-\frac{1}{2}} \nabla \cdot \boldsymbol{v}_D\|_{0,\Omega_D} &\leq \|K^{-\frac{1}{2}} \boldsymbol{v}_D^0\|_{0,\Omega_D} + \|K^{-\frac{1}{2}} \mathcal{R}_D \phi\|_{0,\Omega_D} + \|K^{\frac{1}{2}} w_D\|_{0,\Omega_D} \\
&\lesssim \|K^{-\frac{1}{2}} \nabla \cdot \mathcal{R}_D \phi\|_{0,\Omega_D} + \|K^{-\frac{1}{2}} \mathcal{R}_D \phi\|_{0,\Omega_D} + \|K^{\frac{1}{2}} w_D\|_{0,\Omega_D} \\
&\lesssim \|K^{-\frac{1}{2}} \phi\|_{-\frac{1}{2},\Gamma} + \|K^{\frac{1}{2}} w_D\|_{0,\Omega_D} \\
&\lesssim \|K^{\frac{1}{2}} w_D\|_{0,\Omega_D}.
\end{aligned} \tag{3.11b}$$

In the final step, we have used that $H^1(\Gamma) \subseteq H^{-\frac{1}{2}}(\Gamma)$ and (3.7a).

By construction, $\boldsymbol{v}$ now satisfies the following two properties:

$$\|\boldsymbol{v}\|_V = \left(\|\mu^{\frac{1}{2}} \boldsymbol{v}_S\|_{1,\Omega_S}^2 + \|K^{-\frac{1}{2}} \boldsymbol{v}_D\|_{0,\Omega_D}^2 + \|K^{-\frac{1}{2}} \nabla \cdot \boldsymbol{v}_D\|_{0,\Omega_D}^2 \right)^{\frac{1}{2}} \lesssim \|w\|_W, \tag{3.12a}$$

$$\begin{aligned}
b(\boldsymbol{v}, w) &= -(\nabla \cdot \boldsymbol{v}_S, w_S)_{\Omega_S} - (\nabla \cdot \boldsymbol{v}_D, w_D)_{\Omega_D} \\
&= -(\nabla \cdot (\nabla p_S + \mathcal{R}_S \phi), w_S)_{\Omega_S} - (\nabla \cdot (\nabla p_D + \mathcal{R}_D \phi), w_D)_{\Omega_D} \\
&= \|\mu^{-\frac{1}{2}} w_S\|_{0,\Omega_S}^2 + \|K^{\frac{1}{2}} w_D\|_{0,\Omega_D}^2 \\
&= \|w\|_W^2.
\end{aligned} \tag{3.12b}$$

The proof is concluded by gathering (3.12). □

In the special case of $|\partial_p \Omega_D| > 0$, the Darcy subproblem is itself well-posed. This can be used to our advantage in the proof of (3.3d). In particular, the construction of $\phi \in \Lambda$ becomes obsolete, as shown in the following corollary.

Corollary 3.2. *If $|\partial_p\Omega_D| > 0$, then for each $w \in W$, there exists $\boldsymbol{v}^0 \in \boldsymbol{V}^0$ with $\boldsymbol{v}^0 \neq 0$ such that*

$$b(\boldsymbol{v}^0, w) \gtrsim \|\boldsymbol{v}^0\|_V \|w\|_W.$$

Proof. We follow the same arguments as for (3.3d) in Lemma 3.1. The main difference is that we now set $\phi = 0$ and solve auxiliary Poisson problems to obtain $(\boldsymbol{v}_S^0, \boldsymbol{v}_D^0) \in \boldsymbol{V}_S^0 \times \boldsymbol{V}_D^0$ such that

$$\begin{aligned} -\nabla \cdot \boldsymbol{v}_S^0 &= \mu^{-1} w_S, & -\nabla \cdot \boldsymbol{v}_D^0 &= K w_D, \\ (\boldsymbol{n} \cdot \boldsymbol{v}_S^0)|_{\partial\Omega_S \setminus \partial_\sigma \Omega_S} &= 0, & (\boldsymbol{n} \cdot \boldsymbol{v}_D^0)|_{\partial\Omega_D \setminus \partial_p \Omega_D} &= 0. \end{aligned}$$

Since both $\partial_\sigma\Omega_S$ and $\partial_p\Omega_D$ have positive measure, these two subproblems are well-posed and the statement follows by elliptic regularity. □

We are now ready to present the main result of this section, namely that problem (2.11) is well-posed with respect to the weighted norms of (3.2).

Theorem 3.3. *Problem (2.11) is well-posed, i.e. a unique solution $(\boldsymbol{u}, p) \in \boldsymbol{V} \times W$ exists satisfying*

$$\|\boldsymbol{u}\|_V + \|p\|_W \lesssim \|\mu^{-\frac{1}{2}} \boldsymbol{f}_S\|_{-1,\Omega_S} + \|K^{-\frac{1}{2}} f_D\|_{0,\Omega_D} + \|K^{\frac{1}{2}} g_p\|_{\frac{1}{2},\partial_p\Omega_D}. \tag{3.13}$$

Proof. With the inequalities from Lemma 3.1, it suffices to show continuity of the right-hand side. Let us therefore apply the Cauchy–Schwarz inequality followed by a trace inequality:

$$\begin{aligned} f_u(\boldsymbol{v}) + f_p(w) &= (\boldsymbol{f}_S, \boldsymbol{v}_S)_{\Omega_S} + (f_D, w_D)_{\Omega_D} + (g_p, \boldsymbol{n} \cdot \boldsymbol{v}_D)_{\partial_p\Omega_D} \\ &\leq \|\mu^{-\frac{1}{2}} \boldsymbol{f}_S\|_{-1,\Omega_S} \|\mu^{\frac{1}{2}} \boldsymbol{v}_S\|_{1,\Omega_S} + \|K^{-\frac{1}{2}} f_D\|_{0,\Omega_D} \|K^{\frac{1}{2}} w_D\|_{0,\Omega_D} \\ &\quad + \|K^{\frac{1}{2}} g_p\|_{\frac{1}{2},\partial_p\Omega_D} \|K^{-\frac{1}{2}} \boldsymbol{n} \cdot \boldsymbol{v}_D\|_{-\frac{1}{2},\partial_p\Omega_D} \\ &\lesssim (\|\mu^{-\frac{1}{2}} \boldsymbol{f}_S\|_{-1,\Omega_S} + \|K^{-\frac{1}{2}} f_D\|_{0,\Omega_D} + \|K^{\frac{1}{2}} g_p\|_{\frac{1}{2},\partial_p\Omega_D})(\|\boldsymbol{v}\|_V + \|w\|_W). \end{aligned}$$

With the continuity of the right-hand shown, all requirements are satisfied to invoke standard saddle point theory [5], proving the claim. □

4. The Steklov–Poincaré system

The strategy is to introduce the Steklov–Poincaré operator Σ and reduce the system (2.11) to a problem concerning only the interface flux ϕ. The reason for this is twofold. First, since the interface is a lower-dimensional manifold, the problem is reduced in dimensionality and is therefore expected to be easier to solve. Second, we show that the resulting system is symmetric and positive-definite and hence amenable to a large class of iterative solvers including the Minimal Residual (MinRes) and the Conjugate Gradient (CG) method.

We start with the case in which both the pressure and stress boundary conditions are prescribed on a part of the boundary with positive measure, *i.e.* we assume that $|\partial_\sigma\Omega_S| > 0$ and $|\partial_p\Omega_D| > 0$. The cases in which one, or both, of the subproblems have pure Neumann boundary conditions are considered afterward.

In order to construct the reduced problem, we use the bilinear forms and functionals from (2.12) and the extension operator $\mathcal{R}$ from Section 2.1 and define the operator $\Sigma : \Lambda \to \Lambda^*$ and $\chi \in \Lambda^*$ as

$$\langle \Sigma\phi, \varphi \rangle := a(\boldsymbol{u}_\star^0 + \mathcal{R}\phi, \mathcal{R}\varphi) + b(\mathcal{R}\varphi, p_\star), \tag{4.1a}$$

$$\langle \chi, \varphi \rangle := f_u(\mathcal{R}\varphi) - a(\boldsymbol{u}_0^0, \mathcal{R}\varphi) - b(\mathcal{R}\varphi, p_0), \tag{4.1b}$$

in which $\langle \cdot, \cdot \rangle$ denotes the duality pairing on $\Lambda^* \times \Lambda$. Here, the pair $(\boldsymbol{u}_\star^0, p_\star) \in \boldsymbol{V}^0 \times W$ satisfies

$$a(\boldsymbol{u}_\star^0, \boldsymbol{v}^0) + b(\boldsymbol{v}^0, p_\star) = -a(\mathcal{R}\phi, \boldsymbol{v}^0), \qquad \forall \boldsymbol{v}^0 \in \boldsymbol{V}^0, \tag{4.2a}$$

$$b(\boldsymbol{u}_\star^0, w) = -b(\mathcal{R}\phi, w), \qquad \forall w \in W. \tag{4.2b}$$

and the pair $(\boldsymbol{u}_0^0, p_0) \in \boldsymbol{V}^0 \times W$ is defined such that

$$a(\boldsymbol{u}_0^0, \boldsymbol{v}^0) + b(\boldsymbol{v}^0, p_0) = f_u(\boldsymbol{v}^0), \qquad \forall \boldsymbol{v}^0 \in \boldsymbol{V}^0, \tag{4.3a}$$

$$b(\boldsymbol{u}_0^0, w) = f_p(w), \qquad \forall w \in W. \tag{4.3b}$$

With the above definitions, we introduce the reduced interface problem as:
Find $\phi \in \Lambda$ such that

$$\langle \Sigma\phi, \varphi \rangle = \langle \chi, \varphi \rangle, \qquad \forall \varphi \in \Lambda. \tag{4.4}$$

Note that setting $\boldsymbol{u} := \boldsymbol{u}_\star^0 + \boldsymbol{u}_0^0 + \mathcal{R}\phi$ and $p := p_\star + p_0$ yields the solution to the original problem (2.11). Hence, if this problem admits a unique solution, then (4.4) and (2.11) are equivalent.

Similar to the analysis of problem (2.11) in Section 3, we require an appropriate, parameter-dependent norm on functions $\varphi \in \Lambda$ in order to analyze (4.4). Let us therefore define

$$\|\varphi\|_\Lambda^2 := \|\mu^{\frac{1}{2}}\varphi\|_{\frac{1}{2},\Gamma}^2 + \|K^{-\frac{1}{2}}\varphi\|_{-\frac{1}{2},\Gamma}^2. \tag{4.5}$$

We justify this choice by proving two bounds with respect to $\|\cdot\|_V$ in the following lemma. These results are then used in a subsequent theorem to show that Σ is continuous and coercive with respect to $\|\cdot\|_\Lambda$.

Lemma 4.1. *Given $\phi \in \Lambda$, then the following bounds hold for any $\boldsymbol{u}^0 \in \boldsymbol{V}^0$:*

$$\|\phi\|_\Lambda \lesssim \|\boldsymbol{u}^0 + \mathcal{R}\phi\|_V, \qquad \|\mathcal{R}\phi\|_V \lesssim \|\phi\|_\Lambda. \tag{4.6}$$

Proof. We apply trace inequalities in $H^1(\Omega_S)$ and $H(\mathrm{div}, \Omega_D)$:

$$\begin{aligned}\|\phi\|_\Lambda^2 &= \|\mu^{\frac{1}{2}}\phi\|_{\frac{1}{2},\Gamma}^2 + \|K^{-\frac{1}{2}}\phi\|_{-\frac{1}{2},\Gamma}^2 \\ &\lesssim \|\mu^{\frac{1}{2}}(\boldsymbol{u}_S^0 + \mathcal{R}_S\phi)\|_{1,\Omega_S}^2 + \|K^{-\frac{1}{2}}(\boldsymbol{u}_D^0 + \mathcal{R}_D\phi)\|_{0,\Omega_D}^2 + \|K^{-\frac{1}{2}}\nabla\cdot(\boldsymbol{u}_D^0 + \mathcal{R}_D\phi)\|_{0,\Omega_D}^2 = \|\boldsymbol{u}^0 + \mathcal{R}\phi\|_V^2.\end{aligned}$$

Thus, the first inequality is shown. On the other hand, the continuity of $\mathcal{R}_i$ for $i \in \{S, D\}$ from (2.5) gives us

$$\begin{aligned}\|\mathcal{R}\phi\|_V^2 &\le \|\mu^{\frac{1}{2}}\mathcal{R}_S\phi\|_{1,\Omega_S}^2 + \|K^{-\frac{1}{2}}\mathcal{R}_D\phi\|_{0,\Omega_D}^2 + \|K^{-\frac{1}{2}}\nabla\cdot\mathcal{R}_D\phi\|_{0,\Omega_D}^2 \\ &\lesssim \|\mu^{\frac{1}{2}}\phi\|_{\frac{1}{2},\Gamma}^2 + \|K^{-\frac{1}{2}}\phi\|_{-\frac{1}{2},\Gamma}^2 = \|\phi\|_\Lambda^2.\end{aligned}$$

□

Theorem 4.2. *The operator $\Sigma : \Lambda \to \Lambda^*$ is symmetric, continuous, and coercive with respect to the norm $\|\cdot\|_\Lambda$.*

Proof. We first note that the auxiliary problem (4.2) is well-posed by Lemma 3.1, Corollary 3.2, and saddle point theory. Moreover, the right-hand side is continuous due to (3.3a) and (3.3b). For given ϕ, the pair $(\boldsymbol{u}_\star^0, p_\star)$ therefore exists uniquely and satisfies

$$\|\boldsymbol{u}_\star^0\|_V + \|p_\star\|_W \lesssim \|\mathcal{R}\phi\|_V. \tag{4.7}$$

Symmetry is considered next. Let $(\boldsymbol{u}_\varphi, p_\varphi)$ be the solution to (4.2) with data φ. By setting $(\boldsymbol{v}^0, w) = (\boldsymbol{u}_\star^0, p_\star)$ in the corresponding problem, it follows that

$$a(\boldsymbol{u}_\varphi^0, \boldsymbol{u}_\star^0) + b(\boldsymbol{u}_\star^0, p_\varphi) + b(\boldsymbol{u}_\varphi^0, p_\star) = -a(\mathcal{R}\varphi, \boldsymbol{u}_\star^0) - b(\mathcal{R}\varphi, p_\star).$$

Substituting this in definition (4.1a) and using the symmetry of a, we obtain

$$\langle \Sigma\phi, \varphi \rangle = a(\mathcal{R}\phi, \mathcal{R}\varphi) + a(\boldsymbol{u}_\star^0, \mathcal{R}\varphi) + b(\mathcal{R}\varphi, p_\star) = a(\mathcal{R}\phi, \mathcal{R}\varphi) - a(\boldsymbol{u}_\star^0, \boldsymbol{u}_\varphi^0) - b(\boldsymbol{u}_\varphi^0, p_\star) - b(\boldsymbol{u}_\star^0, p_\varphi), \tag{4.8}$$

and symmetry of Σ is shown.

We continue by proving continuity of Σ. Employing (3.3a) and (3.3b) once again, it follows that

$$\langle \Sigma\phi, \varphi\rangle \lesssim (\|\boldsymbol{u}_\star^0\|_V + \|\mathcal{R}\phi\|_V + \|p_\star\|_W)\|\mathcal{R}\varphi\|_V \lesssim \|\mathcal{R}\phi\|_V\|\mathcal{R}\varphi\|_V \lesssim \|\phi\|_\Lambda\|\varphi\|_\Lambda \tag{4.9}$$

in which the second and third inequalities follow from (4.7) and Lemma 4.1, respectively.

It remains to show coercivity, which we derive by setting $\varphi = \phi$ and $(\boldsymbol{v}^0, w) = (\boldsymbol{u}_\star^0, p_\star)$ in (4.2):

$$\langle \Sigma\phi, \phi\rangle = a(\boldsymbol{u}_\star^0 + \mathcal{R}\phi, \mathcal{R}\phi) + b(\mathcal{R}\phi, p_\star) = a(\boldsymbol{u}_\star^0 + \mathcal{R}\phi, \mathcal{R}\phi) + a(\boldsymbol{u}_\star^0 + \mathcal{R}\phi, \boldsymbol{u}_\star^0) = a(\boldsymbol{u}_\star^0 + \mathcal{R}\phi, \boldsymbol{u}_\star^0 + \mathcal{R}\phi). \tag{4.10}$$

Next, we observe that (4.2b) gives us $b(\boldsymbol{u}_\star^0 + \mathcal{R}\phi, w) = 0$ for all $w \in W$. Thus, we use (3.3c) and Lemma 4.1 to conclude that

$$\langle \Sigma\phi, \phi\rangle \gtrsim \|\boldsymbol{u}_\star^0 + \mathcal{R}\phi\|_V^2 \gtrsim \|\phi\|_\Lambda^2. \tag{4.11}$$

□

Corollary 4.3. *Problem (4.4) is well-posed and the solution $\phi \in \Lambda$ satisfies*

$$\|\phi\|_\Lambda \lesssim \|\mu^{-\frac{1}{2}}\boldsymbol{f}_S\|_{-1,\Omega_S} + \|K^{-\frac{1}{2}}f_D\|_{0,\Omega_D} + \|K^{\frac{1}{2}}g_p\|_{\frac{1}{2},\partial_p\Omega_D}. \tag{4.12}$$

Proof. As shown in Theorem 4.2, Σ is symmetric and positive-definite. Therefore, (4.4) admits a unique solution. We then set $\boldsymbol{u} = \boldsymbol{u}_\star^0 + \boldsymbol{u}_0^0 + \mathcal{R}\phi$ and $p = p_\star + p_0$ and note that $(\boldsymbol{u}, p)$ is the solution to (2.11). By employing Lemma 4.1, we note that $\|\phi\|_\Lambda \lesssim \|\boldsymbol{u}\|_V + \|p\|_W$ and the proof is concluded using the result from Theorem 3.3. □

4.1. Neumann problems

In this section, we consider the case in which one, or both, of the subproblems have flux boundary conditions prescribed on the entire boundary. In other words, the cases in which $|\partial_\sigma\Omega_S| = 0$ or $|\partial_p\Omega_D| = 0$. We first introduce the setting in which one of the subdomains corresponds to a Neumann problem, followed by the case of $|\partial_\sigma\Omega_S| = |\partial_p\Omega_D| = 0$.

4.1.1. Single Neumann subproblem

Let us consider $|\partial_p\Omega_D| = 0$ and $|\partial_\sigma\Omega_S| > 0$, noting that the converse case follows by symmetry. The complication in this case is that solving the Darcy subproblem results in a pressure distribution that is defined up to a constant. Thus, several preparatory steps need to be made before the interface problem can be formulated and solved.

The key idea is to pose the interface problem on the subspace of Λ containing functions with zero mean. This is done by introducing a function $\phi_\star$ that balances the source term in Ω_D and subtracting this from the problem. The modified interface problem produces a pressure distribution with zero mean in Ω_D and we obtain the true pressure average obtained afterwards.

Let us first define the subspace $\Lambda_0 \subset \Lambda$ of functions with zero mean, *i.e.*

$$\Lambda_0 := \{\varphi_0 \in \Lambda : \ (\varphi_0, 1)_\Gamma = 0\}. \tag{4.13}$$

We continue by constructing $\phi_\star \in \Lambda \setminus \Lambda_0$. For that, we follow Section 5.3 of [30] and introduce $\zeta \in \Lambda$ as an interface flux with non-zero mean. For convenience, we choose ζ such that

$$(\zeta, 1)_\Gamma = 1. \tag{4.14}$$

Any bounded ζ with this property will suffice for our purposes. As a concrete example, we uniquely define ζ by solving a minimization problem in $H_0^1(\Gamma)$ with (4.14) as a constraint, similar to the construction (3.6) in Lemma 3.1.

Next, we test the mass conservation equation (2.11b) with $w = 1_{\Omega_D}$, the indicator function of Ω_D. Due to the assumption $|\partial_p \Omega_D| = 0$, the divergence theorem gives us

$$f_p(1_{\Omega_D}) = -(f_D, 1)_{\Omega_D} = -(\nabla \cdot (\boldsymbol{u}_D^0 + \mathcal{R}_D\phi), 1)_{\Omega_D} = (\phi, 1)_\Gamma.$$

Using this observation, we define the function $\phi_\star \in \Lambda \setminus \Lambda_0$ such that $(\phi_\star, 1)_\Gamma = (\phi, 1)_\Gamma$ by setting

$$\phi_\star := \zeta f_p(1_{\Omega_D}). \tag{4.15}$$

The next step is to pose the interface problem, similar to (4.4), in this subspace:
Find $\phi_0 \in \Lambda_0$ such that

$$\langle \Sigma\phi_0, \varphi_0 \rangle = \langle \chi, \varphi_0 \rangle, \qquad \forall \varphi_0 \in \Lambda_0, \tag{4.16}$$

with $\Sigma : \Lambda \to \Lambda^*$ and $\chi \in \Lambda^*$ redefined as

$$\langle \Sigma\phi_0, \varphi_0 \rangle := a(\boldsymbol{u}_0^0 + \mathcal{R}\phi_0, \mathcal{R}\varphi_0) + b(\mathcal{R}\varphi_0, p_0), \tag{4.17a}$$

$$\langle \chi, \varphi_0 \rangle := f_u(\mathcal{R}\varphi_0) - a(\boldsymbol{u}_\star^0 + \mathcal{R}\varphi_\star, \mathcal{R}\varphi_0) - b(\mathcal{R}\varphi_0, p_\star). \tag{4.17b}$$

The construction of the pairs $(\boldsymbol{u}_\star^0, p_\star)$ and $(\boldsymbol{u}_0^0, p_0)$ now require solving the Darcy subproblem with pure Neumann conditions. We emphasize that due to the nature of these problems, the pressure distributions are defined up to a constant and we therefore enforce $p_\star$ and p_0 to have mean zero with the use of Lagrange multipliers.

In particular, let $(\boldsymbol{u}_0^0, p_0, r_0) \in \boldsymbol{V}^0 \times W \times \mathbb{R}$ satisfy the following:

$$a(\boldsymbol{u}_0^0, \boldsymbol{v}^0) + b(\boldsymbol{v}^0, p_0) = -a(\mathcal{R}\phi_0, \boldsymbol{v}^0), \qquad \forall \boldsymbol{v}^0 \in \boldsymbol{V}^0, \tag{4.18a}$$

$$(r_0, w)_{\Omega_D} + b(\boldsymbol{u}_0^0, w) = -b(\mathcal{R}\phi_0, w), \qquad \forall w \in W, \tag{4.18b}$$

$$(p_0, s)_{\Omega_D} = 0, \qquad \forall s \in \mathbb{R}. \tag{4.18c}$$

Similarly, we let $(\boldsymbol{u}_\star^0, p_\star, r_\star) \in \boldsymbol{V}^0 \times W \times \mathbb{R}$ solve

$$a(\boldsymbol{u}_\star^0, \boldsymbol{v}^0) + b(\boldsymbol{v}^0, p_\star) = -a(\mathcal{R}\phi_\star, \boldsymbol{v}^0) + f_u(\boldsymbol{v}^0), \qquad \forall \boldsymbol{v}^0 \in \boldsymbol{V}^0, \tag{4.19a}$$

$$(r_\star, w)_{\Omega_D} + b(\boldsymbol{u}_\star^0, w) = -b(\mathcal{R}\phi_\star, w) + f_p(w), \qquad \forall w \in W, \tag{4.19b}$$

$$(p_\star, s)_{\Omega_D} = 0, \qquad \forall s \in \mathbb{R}. \tag{4.19c}$$

We emphasize that setting $w = 1_{\Omega_D}$ in the conservation equations (4.18b) and (4.19b) yields $r_\star = r_0 = 0$. Hence, these terms have no contribution to the mass balance.

The solution to problem (4.16) allows us to construct the velocity distribution:

$$\boldsymbol{u} := \boldsymbol{u}_0^0 + \boldsymbol{u}_\star^0 + \mathcal{R}(\phi_0 + \phi_\star). \tag{4.20}$$

The next step is to recover the correct pressure average in Ω_D. For that, we presume that the pressure solution is given by $p = p_0 + p_\star + \bar{p}$ with $\bar{p} := c_D 1_{\Omega_D}$ for some $c_D \in \mathbb{R}$. In other words, $\bar{p}$ is zero in Ω_S and a constant c_D on Ω_D, to be determined next.

Using ζ from (4.14), we substitute this function in (2.11a) and choose the test function $\boldsymbol{v} = \mathcal{R}\zeta$:

$$a(\boldsymbol{u}, \mathcal{R}\zeta) + b(\mathcal{R}\zeta, p_0 + p_\star + \bar{p}) = f_u(\mathcal{R}\zeta).$$

Using this relationship and the divergence theorem, we make the following two observations:

$$b(\mathcal{R}\zeta, \bar{p}) = f_u(\mathcal{R}\zeta) - a(\boldsymbol{u}, \mathcal{R}\zeta) - b(\mathcal{R}\zeta, p_0 + p_\star) = \langle \chi - \Sigma\phi_0, \zeta \rangle, \tag{4.21a}$$

$$b(\mathcal{R}\zeta, \bar{p}) = -(\nabla \cdot \mathcal{R}\zeta, \bar{p})_{\Omega_D} = c_D(\zeta, 1)_\Gamma = c_D. \tag{4.21b}$$

Combining these two equations yields $c_D = \langle \chi - \Sigma\phi_0, \zeta \rangle$ and we set

$$\bar{p} := \langle \chi - \Sigma\phi_0, \zeta \rangle 1_{\Omega_D}. \tag{4.22}$$

Finally, by setting $p := p_0 + p_\star + \bar{p}$, we have obtained $(\boldsymbol{u}, p) \in \boldsymbol{V} \times W$, the solution to (2.11). We remark that the well-posedness of (4.16) follows by the same arguments as in Theorem 4.2.

4.1.2. Coupled Neumann problems

In this case, we have flux conditions prescribed on the entire boundary, *i.e.* $\partial\Omega = \partial_u\Omega_S \cup \partial_u\Omega_D$. We follow the same steps as in Section 4.1.1, and highlight the differences required to treat this case.

Let us consider a slightly more general case than (2.12) by including a source function f_S in the Stokes subdomain. In other words, the right-hand side of the mass balance equations is given by

$$f_p(w) := -(f_S, w_S)_{\Omega_S} - (f_D, w_D)_{\Omega_D}. \tag{4.23}$$

By compatibility of the source function with the boundary conditions, it follows that $f_p(1) = 0$ and therefore

$$f_p(1_{\Omega_D}) = (f_D, 1)_{\Omega_D} = -(f_S, 1)_{\Omega_S} = -f_p(1_{\Omega_S}). \tag{4.24}$$

Let $\Lambda_0 \subset \Lambda$ be defined as in (4.13) and ζ as in (4.14). Using the same arguments as in the previous section, we define

$$\phi_\star := \zeta f_p(1_{\Omega_D}) = -\zeta f_p(1_{\Omega_S}). \tag{4.25}$$

The operators Σ and χ are defined as in (4.17) with the only difference being in the pairs of functions $(\boldsymbol{u}_0^0, p_0)$ and $(\boldsymbol{u}_\star^0, p_\star)$. As before, these pairs are constructing by solving the separate subproblems. Since these correspond to Neumann problems, it follows that the pressure distributions p_0 and $p_\star$ are defined up to a constant in each subdomain. We therefore enforce zero mean of these variables in each subdomain with the use of a Lagrange multiplier $s \in S$. Let S be the space of piecewise constant functions given by

$$S := \operatorname{span}\{1_{\Omega_S}, 1_{\Omega_D}\}. \tag{4.26}$$

We augment problem (4.18) to:
Find $(\boldsymbol{u}_0^0, p_0, r_0) \in \boldsymbol{V}^0 \times W \times S$ such that

$$a(\boldsymbol{u}_0^0, \boldsymbol{v}^0) + b(\boldsymbol{v}^0, p_0) = -a(\mathcal{R}\phi_0, \boldsymbol{v}^0), \qquad \forall \boldsymbol{v}^0 \in \boldsymbol{V}^0, \tag{4.27a}$$

$$(r_0, w)_\Omega + b(\boldsymbol{u}_0^0, w) = -b(\mathcal{R}\phi_0, w), \qquad \forall w \in W, \tag{4.27b}$$

$$(p_0, s)_\Omega = 0, \qquad \forall s \in S. \tag{4.27c}$$

Problem (4.19) is changed analogously to produce $(\boldsymbol{u}_\star^0, p_\star, r_\star) \in \boldsymbol{V}^0 \times W \times S$. After solving the interface problem, all ingredients are available to construct the velocity $\boldsymbol{u}$ as in (4.20).

In the construction of the pressure p, we compute $c_D = \langle \chi - \Sigma\phi_0, \zeta \rangle$ using the same arguments as in (4.21). Since the pressure is globally defined up to a constant, we ensure that the pressure distribution has mean zero on Ω by setting

$$\bar{p} := \langle \chi - \Sigma\phi_0, \zeta \rangle \left(1_{\Omega_D} - \frac{|\Omega_D|}{|\Omega|} \right). \tag{4.28}$$

As before, we set $p := p_0 + p_\star + \bar{p}$ and obtain the solution $(\boldsymbol{u}, p)$ of the original problem (2.11).

5. Discretization

This section presents the discretization of problem (2.11) with the use of the Mixed Finite Element method. By introducing the interface flux as a separate variable, we derive a mortar method reminiscent of [6, 29], presented in the context of fracture flow. The focus in this section is to introduce this flux-mortar method for the coupled Stokes–Darcy problem and show its stability.

Let $\Omega_{S,h}$, $\Omega_{D,h}$, Γ_h be shape-regular tesselations of Ω_S, Ω_D, and Γ, respectively. Let $\Omega_{S,h}$ and $\Omega_{D,h}$ be constructed independently and consist of simplicial or quadrangular (hexahedral in 3D) elements. Similarly, Γ_h is a simplicial or quadrangular mesh of dimension $n-1$, constructed according to the restrictions mentioned below.

We impose the following three restriction on the Mixed Finite Element discretization:

(1) For the purpose of structure preservation, the finite element spaces are chosen such that

$$\boldsymbol{V}_{S,h} \subset \boldsymbol{V}_S, \qquad \boldsymbol{V}_{D,h} \subset \boldsymbol{V}_D, \qquad \Lambda_h \subset \Lambda, \tag{5.1a}$$

$$W_{S,h} \subset W_S, \qquad W_{D,h} \subset W_D. \tag{5.1b}$$

It is convenient, but not necessary, to define Γ_h as the trace mesh of $\Omega_{S,h}$ and $\Lambda_h = (\boldsymbol{n} \cdot \boldsymbol{V}_{S,h})|_\Gamma$. In this case, it follows that $\Lambda_h \subset H_0^1(\Gamma) \subset H_{00}^{1/2}(\Gamma) = \Lambda$. We moreover define

$$\boldsymbol{V}_{S,h}^0 := \boldsymbol{V}_{S,h} \cap \boldsymbol{V}_S^0, \qquad \boldsymbol{V}_{D,h}^0 := \boldsymbol{V}_{D,h} \cap \boldsymbol{V}_D^0. \tag{5.2}$$

(2) The Mixed Finite Element spaces $V_{i,h} \times W_{i,h}$ with $i \in \{S, D\}$ are chosen to form stable pairs for the Stokes and Darcy (sub)systems, respectively. In particular, bounded interpolation operators Π_{V_i} exist for $i \in \{S, D\}$ such that for all $\boldsymbol{v} \in \boldsymbol{V} \cap H^\epsilon(\Omega)$ with $\epsilon > 0$:

$$\Pi_{W_S} \nabla \cdot ((I - \Pi_{V_S})\boldsymbol{v}_S) = 0, \qquad \nabla \cdot (\Pi_{V_D} \boldsymbol{v}_D) = \Pi_{W_D} \nabla \cdot \boldsymbol{v}_D, \tag{5.3}$$

in which Π_{W_i} is the L^2-projection onto $W_{i,h}$. Moreover, to ensure local mass conservation, we assume that the space of piecewise constants (P_0) is contained in W_h.

Examples for the Stokes subproblem include $\boldsymbol{P}_2 - P_0$ in the two-dimensional case as well as the Bernardi–Raugel pair [4]. For the Darcy subproblem, stable choices of low-order finite elements include the Raviart–Thomas pair $\mathrm{RT}_0 - P_0$ [31] and the Brezzi–Douglas–Marini pair $\mathrm{BDM}_1 - P_0$ [7]. For more examples of stable Mixed Finite Element pairs, we refer the reader to [5].

(3) For $\phi_h \in \Lambda_h$, let the discrete extension operators $\mathcal{R}_{i,h} : \Lambda_h \to \boldsymbol{V}_{i,h}$ with $i \in \{S, D\}$ satisfy

$$(\phi_h - \boldsymbol{n} \cdot \mathcal{R}_{i,h}\phi_h, \boldsymbol{n} \cdot \boldsymbol{v}_{i,h})_\Gamma = 0, \qquad \forall \boldsymbol{v}_{i,h} \in \boldsymbol{V}_{i,h}. \tag{5.4}$$

The extension operators are continuous in the sense that for $\phi_h \in \Lambda_h$, we have

$$\|\mathcal{R}_{S,h}\varphi_h\|_{1,\Omega_S} \lesssim \|\varphi_h\|_{\frac{1}{2},\Gamma}, \qquad \|\mathcal{R}_{D,h}\varphi_h\|_{0,\Omega_D} + \|\nabla \cdot \mathcal{R}_D\varphi_h\|_{0,\Omega_D} \lesssim \|\varphi_h\|_{-\frac{1}{2},\Gamma}. \tag{5.5}$$

We define $\mathcal{R}_h\phi = \mathcal{R}_{S,h} \oplus \mathcal{R}_{D,h}$Let the mesh Γ_h and function space Λ_h be chosen such that the kernel of $\mathcal{R}_h$ is zero:

$$\mathcal{R}_h\phi_h = 0 \text{ if and only if } \phi_h = 0. \tag{5.6}$$

We remark that this is a common restriction encountered in mortar methods (see *e.g.* [1]) and can be satisfied by choosing Γ_h sufficiently coarse or constructing Λ_h using polynomials of lower order.

With the above restrictions in place, we define the discretizations of the combined spaces $\boldsymbol{V}$ and W as

$$\boldsymbol{V}_h := \left\{\boldsymbol{v}_h : \exists(\boldsymbol{v}_{S,h}^0, \varphi_h, \boldsymbol{v}_{D,h}^0) \in \boldsymbol{V}_{S,h}^0 \times \Lambda_h \times \boldsymbol{V}_{D,h}^0 \text{ s.t. } \boldsymbol{v}_h|_{\Omega_i} = \boldsymbol{v}_{i,h}^0 + \mathcal{R}_{i,h}\varphi_h, \text{ for } i \in \{S, D\}\right\}, \tag{5.7a}$$

$$W_h := W_{S,h} \times W_{D,h}. \tag{5.7b}$$

As in the continuous case, the function space $\boldsymbol{V}_h$ is independent of the choice of extension operators. We remark that in the case of non-matching grids or if different polynomial orders are chosen for $\boldsymbol{V}_{S,h}$ and $\boldsymbol{V}_{D,h}$, we have $V_h \not\subset V$ due to the weaker property of $\mathcal{R}_h$ in (5.4) as opposed to $\mathcal{R}$ defined by (2.4). Nevertheless, a normal flux continuity is imposed in the sense that the normal trace of $\boldsymbol{v}_{S,h}$ and $\boldsymbol{v}_{D,h}$ are L^2 projections of a single variable ϕ_h.

Again, the subscript $i \in \{S, D\}$ distinguishes the restrictions of $(\boldsymbol{v}, w) \in \boldsymbol{V}_h \times W_h$ to the different subdomains:

$$\boldsymbol{v}_{i,h} := \boldsymbol{v}_{i,h}^0 + \mathcal{R}_{i,h}\varphi_h \in \boldsymbol{V}_{i,h}, \qquad w_{i,h} := w_h|_{\Omega_i} \in W_{i,h}. \tag{5.8}$$

We finish this section by formally stating the discrete problem:
Find the pair $(\boldsymbol{u}_h, p_h) \in \boldsymbol{V}_h \times W_h$ such that

$$a(\boldsymbol{u}_h, \boldsymbol{v}_h) + b(\boldsymbol{v}_h, p_h) = f_u(\boldsymbol{v}_h), \qquad \forall \boldsymbol{v}_h \in \boldsymbol{V}_h, \tag{5.9a}$$

$$b(\boldsymbol{u}_h, w_h) = f_p(w_h), \qquad \forall w_h \in W_h. \tag{5.9b}$$

with the bilinear forms and functionals defined in (2.12).

With the chosen spaces, the discretizations on $\Omega_{S,h}$ and $\Omega_{D,h}$ are stable and consistent for the Stokes and Darcy subproblems, respectively. However, in order to show stability of the method for the fully coupled problem (5.9), we briefly confirm that the relevant inequalities hold independent of the mesh parameter h.

Lemma 5.1. *The following inequalities are satisfied:*

$$\text{For } \boldsymbol{u}_h, \boldsymbol{v}_h \in \boldsymbol{V}_h: \qquad a(\boldsymbol{u}_h, \boldsymbol{v}_h) \lesssim \|\boldsymbol{u}_h\|_V \|\boldsymbol{v}_h\|_V. \tag{5.10a}$$

$$\text{For } (\boldsymbol{v}_h, w_h) \in \boldsymbol{V}_h \times W_h: \qquad b(\boldsymbol{v}_h, w_h) \lesssim \|\boldsymbol{v}_h\|_V \|w_h\|_W. \tag{5.10b}$$

$$\text{For } \boldsymbol{v}_h \in \boldsymbol{V}_h \text{ with } b(\boldsymbol{v}_h, w_h) = 0 \ \forall w_h \in W_h: \qquad a(\boldsymbol{v}_h, \boldsymbol{v}_h) \gtrsim \|\boldsymbol{v}_h\|_V^2. \tag{5.10c}$$

$$\text{For } w_h \in W_h, \ \exists \boldsymbol{v}_h \in \boldsymbol{V}_h \text{ with } \boldsymbol{v}_h \neq 0, \text{ such that}: \qquad b(\boldsymbol{v}_h, w_h) \gtrsim \|\boldsymbol{v}_h\|_V \|w_h\|_W. \tag{5.10d}$$

Proof. Inequalities (5.10a) and (5.10b) follow using the same arguments as (3.4) in Lemma 3.1. Continuing with (5.10c), we note from (5.3) that $b(\boldsymbol{v}_h, w_h) = 0$ implies

$$0 = \Pi_{W_D} \nabla \cdot \boldsymbol{v}_{D,h} = \nabla \cdot (\Pi_{V_D} \boldsymbol{v}_{D,h}) = \nabla \cdot \boldsymbol{v}_{D,h}.$$

Hence, the same derivation as (3.5) is followed to give us (5.10c).

For the final inequality, we consider $w_h \in W_h$ given and follow the strategy of Lemma 3.1. First, we set up a minimization problem in Λ_h analogous to (3.6) to obtain a bounded $\phi_h \in \Lambda_h$ such that

$$\|\phi_h\|_{1,\Gamma} \lesssim \|K w_{D,h}\|_{0,\Omega_D}, \tag{5.11a}$$

$$(\nabla \cdot \mathcal{R}_{D,h}\phi_h, 1)_{\Omega_D} = (-\boldsymbol{n} \cdot \mathcal{R}_{D,h}\phi_h, 1)_\Gamma = (-\phi_h, 1)_\Gamma = -(K w_{D,h}, 1)_{\Omega_D}. \tag{5.11b}$$

Next, we note that $w_h \in W_h \subset W$. In turn, we use the auxiliary problems (3.8) and (3.9) to construct $\boldsymbol{v}_S^0 \in \boldsymbol{V}_S^0$ and $\boldsymbol{v}_D^0 \in \boldsymbol{V}_D^0$ such that

$$-\nabla \cdot \boldsymbol{v}_S^0 = \mu^{-1} w_{S,h} + \nabla \cdot \mathcal{R}_{S,h}\phi_h, \tag{5.12a}$$

$$-\nabla \cdot \boldsymbol{v}_D^0 = K w_{D,h} + \nabla \cdot \mathcal{R}_{D,h}\phi_h, \tag{5.12b}$$

$$\|\boldsymbol{v}_S^0\|_{1,\Omega_S} \lesssim \|\mu^{-1} w_{S,h}\|_{0,\Omega_S} + \|\nabla \cdot \mathcal{R}_{S,h}\phi_h\|_{0,\Omega_S}, \tag{5.12c}$$

$$\|\boldsymbol{v}_D^0\|_{1,\Omega_D} \lesssim \|K w_{D,h}\|_{0,\Omega_D} + \|\nabla \cdot \mathcal{R}_{D,h}\phi_h\|_{0,\Omega_D}. \tag{5.12d}$$

We then employ the interpolation operators from (5.3) to create $\boldsymbol{v}_{S,h}^0 = \Pi_{V_S} \boldsymbol{v}_S^0$ and $\boldsymbol{v}_{D,h}^0 = \Pi_{V_D} \boldsymbol{v}_D^0$. Using the commutative properties, we obtain

$$b(\boldsymbol{v}_h, w_h) = -\sum_{i \in \{S,D\}} (\nabla \cdot (\Pi_{V_i} \boldsymbol{v}_i^0 + \mathcal{R}_{i,h}\phi_h), w_{i,h})_{\Omega_i} = (\mu^{-1} w_{S,h}, w_{S,h})_{\Omega_S} + (K w_{D,h}, w_{D,h})_{\Omega_D} = \|w_h\|_W^2.$$

Moreover, by the boundedness of these interpolation operators, we have

$$\|\boldsymbol{v}_h\|_V \leq \|\boldsymbol{v}_h^0\|_V + \|\mathcal{R}_h\phi_h\|_V \lesssim \|\boldsymbol{v}^0\|_V + \|\phi_h\|_\Lambda \lesssim \|w_h\|_W,$$

proving the final inequality (5.10d). □

Theorem 5.2. *If the three conditions presented at the beginning of this section are satisfied, then the discretization method is stable, i.e. a unique solution* $(\boldsymbol{u}_h, p_h) \in \boldsymbol{V}_h \times W_h$ *exists for* (5.9) *satisfying*

$$\|\boldsymbol{u}_h\|_V + \|p_h\|_W \lesssim \|\mu^{-\frac{1}{2}} \boldsymbol{f}_S\|_{-1,\Omega_S} + \|K^{-\frac{1}{2}} f_D\|_{0,\Omega_D} + \|K^{\frac{1}{2}} g_p\|_{\frac{1}{2},\partial_p\Omega_D}. \tag{5.13}$$

Proof. This result follows from Lemma 5.1, the continuity of the right-hand side from Theorem 3.3, and saddle point theory. □

6. Iterative solution method

With well-posedness of the discrete system shown in the previous section, we continue by constructing an efficient solution method to solve the coupled system in an iterative manner. The scheme is introduced according to three steps. We first present the discrete Steklov–Poincaré system that we aim to solve using a Krylov subspace method. Second, a parameter-robust preconditioner is introduced for the reduced system. The third step combines these two ideas to form an iterative method that respects mass conservation at each iteration.

6.1. Discrete Steklov–Poincaré system

Similar to the continuous case in Section 4, we reduce the problem to the interface flux variables $\phi_h \in \Lambda_h$. The reduced system is a direct translation of (4.4) to the discrete setting:
Find $\phi_h \in \Lambda_h$ such that

$$\langle \Sigma_h \phi_h, \varphi_h \rangle = \langle \chi_h, \varphi_h \rangle, \qquad \forall \varphi_h \in \Lambda_h. \tag{6.1}$$

To ease the implementation of the scheme, we focus particularly on the structure of the operator Σ_h. For that, we note that the space $\boldsymbol{V}_h^0$ can be decomposed orthogonally into $\boldsymbol{V}_{S,h}^0 \times \boldsymbol{V}_{D,h}^0$ and a similar decomposition holds for W_h. The aim is to propose a solution method which exploits this property. For brevity, the subscript h is omitted on all variables and operators, keeping in mind that the remainder of this section concerns the discretized setting.

Let us rewrite the bilinear forms a and b in terms of duality pairings, thereby revealing the matrix structure of the problem. For that, we group the terms according to the subdomains and let the operators $A_i : \boldsymbol{V}_{i,h} \to \boldsymbol{V}_{i,h}^*$ and $B_i : \boldsymbol{V}_{i,h} \to W_{i,h}^*$ be defined for $i \in \{S, D\}$ such that

$$\begin{aligned}
\langle A_S \boldsymbol{u}_S, \boldsymbol{v}_S \rangle &= (\mu \varepsilon(\boldsymbol{u}_S), \varepsilon(\boldsymbol{v}_S))_{\Omega_S} + (\beta \boldsymbol{\tau} \cdot \boldsymbol{u}_S, \boldsymbol{\tau} \cdot \boldsymbol{v}_S)_\Gamma, \\
\langle A_D \boldsymbol{u}_D, \boldsymbol{v}_D \rangle &= (K^{-1} \boldsymbol{u}_D, \boldsymbol{v}_D)_{\Omega_D}, \\
\langle B_S \boldsymbol{u}_S, w_S \rangle &= -(\nabla \cdot \boldsymbol{u}_S, w_S)_{\Omega_S}, \\
\langle B_D \boldsymbol{u}_D, w_D \rangle &= -(\nabla \cdot \boldsymbol{u}_D, w_D)_{\Omega_D}.
\end{aligned}$$

Let $A_{i,0}$ and $B_{i,0}$ be the respective restrictions of the above to the subspace $\boldsymbol{V}_{i,h}^0$. With these operators and the decomposition $\boldsymbol{u}_i = \boldsymbol{u}_i + \mathcal{R}_i \phi$ for the trial and test functions, problem (2.11) attains the following matrix form:

$$\begin{bmatrix}
A_{S,0} & B_{S,0}^T & & & A_S \mathcal{R}_S \\
B_{S,0} & & & & B_S \mathcal{R}_S \\
 & & A_{D,0} & B_{D,0}^T & A_D \mathcal{R}_D \\
 & & B_{D,0} & & B_D \mathcal{R}_D \\
(A_S \mathcal{R}_S)^T & (B_S \mathcal{R}_S)^T & (A_D \mathcal{R}_D)^T & (B_D \mathcal{R}_D)^T & \sum_i \mathcal{R}_i^T A_i \mathcal{R}_i
\end{bmatrix}
\begin{bmatrix} \boldsymbol{u}_S^0 \\ p_S \\ \boldsymbol{u}_D^0 \\ p_D \\ \phi \end{bmatrix}
=
\begin{bmatrix} f_{S,u} \\ f_{S,p} \\ f_{D,u} \\ f_{D,p} \\ f_\phi \end{bmatrix}. \tag{6.2}$$

In practice, the discrete extension operators are chosen to only have support in the elements adjacent to Γ, leading to a favorable sparsity pattern. We moreover note that the final row corresponds to test functions $\varphi \in \Lambda_h$. The right-hand side of (6.2) is defined such that

$$\langle f_{S,u}, \boldsymbol{v}_S^0 \rangle + \langle f_{S,p}, w_S \rangle + \langle f_{D,u}, \boldsymbol{v}_D^0 \rangle + \langle f_{D,p}, w_D \rangle + \langle f_\phi, \varphi \rangle = f_u(\boldsymbol{v}) + f_p(w), \qquad \forall (\boldsymbol{v}, w) \in \boldsymbol{V}_h \times W_h. \tag{6.3}$$

The discrete Steklov–Poincaré system is obtained by taking a Schur-complement of this system. In particular, we obtain Σ_h and the right-hand side χ_h as

$$\Sigma_h := \sum_{i\in\{S,D\}} \mathcal{R}_i^T A_i \mathcal{R}_i - \mathcal{R}_i^T \begin{bmatrix} A_i & B_i^T \end{bmatrix} \begin{bmatrix} A_{i,0} & B_{i,0}^T \\ B_{i,0} & \end{bmatrix}^{-1} \begin{bmatrix} A_i \\ B_i \end{bmatrix} \mathcal{R}_i, \tag{6.4a}$$

$$\chi_h := f_\phi - \sum_{i\in\{S,D\}} \mathcal{R}_i^T \begin{bmatrix} A_i & B_i^T \end{bmatrix} \begin{bmatrix} A_{i,0} & B_{i,0}^T \\ B_{i,0} & \end{bmatrix}^{-1} \begin{bmatrix} f_{u,i} \\ f_{p,i} \end{bmatrix}. \tag{6.4b}$$

We employ a Krylov subspace method to solve (6.1) iteratively, thereby avoiding the computationally costly assembly of Σ_h. In order to obtain a parameter-robust iterative method, the next step is to introduce an appropriate preconditioner, as presented in the next section.

6.2. Parameter-robust preconditioning

In this section, we construct the preconditioner such that the resulting iterative method is robust with respect to the material parameters (K and μ) and the mesh size (h). For that, we use the parameter-dependent norm $\|\cdot\|_\Lambda$ from (4.5) and follow the framework presented by [26] to form a norm-equivalent preconditioner. In particular, we use the following result from that work:

Lemma 6.1. *Given a bounded, symmetric, positive-definite operator $\Sigma : \Lambda \to \Lambda^*$ and a symmetric positive definite operator $\mathcal{P} : \Lambda^* \to \Lambda$. If the induced norm $\|\phi\|_{\mathcal{P}^{-1}}^2 := \langle \mathcal{P}^{-1}\phi, \phi\rangle$ satisfies*

$$\|\phi\|_\Lambda^2 \lesssim \|\phi\|_{\mathcal{P}^{-1}}^2 \lesssim \|\phi\|_\Lambda^2, \tag{6.5}$$

then $\mathcal{P}$ is a robust preconditioner in the sense that the condition number of $\mathcal{P}\Sigma$ is bounded independent of the material and mesh parameters.

Note that symmetry of Σ_h is apparent from (6.4a). Positive definiteness follows using the same arguments as in Theorem 4.2. The next step is therefore to create an operator $\mathcal{P}^{-1}$ that generates a norm which is equivalent to $\|\cdot\|_\Lambda$ on Λ_h. Recall from (4.5) that $\|\cdot\|_\Lambda$ is composed of fractional Sobolev norms. The key idea is to introduce a matrix $\mathsf{H}(s)$ that induces a norm which is equivalent to $H^s(\Gamma)$ for $s = \pm\frac{1}{2}$. We apply the strategy explained in [22] to achieve this, of which a short description follows.

For given basis $\{\phi_i\}_{i=1}^{n_\Lambda} \in \Lambda_h$ with n_Λ the dimension of Λ_h, let the mass matrix M and stiffness matrix A be defined such that

$$\begin{aligned} \mathsf{M}_{ij} &:= (\phi_j, \phi_i)_\Gamma, \\ \mathsf{A}_{ij} &:= (\nabla_\Gamma \phi_j, \nabla_\Gamma \phi_i)_\Gamma. \end{aligned} \tag{6.6}$$

Then, a complete set of eigenvectors $\mathsf{v}_i \in \mathbb{R}^{n_\Lambda}$ and eigenvalues $\lambda_i \in \mathbb{R}$ exist solving the generalized eigenvalue problem

$$\mathsf{A}\mathsf{v}_i = \lambda_i \mathsf{M}\mathsf{v}_i. \tag{6.7}$$

The eigenvectors satisfy $\mathsf{v}_i^\mathsf{T}\mathsf{M}\mathsf{v}_j = \delta_{ij}$ with δ_{ij} the Kronecker delta function. Let the diagonal matrix $\mathsf{\Lambda} := \mathrm{diag}([\lambda_i]_{i=1}^{n_\Lambda})$ and let V be the matrix with v_i as its columns. The following eigendecomposition then holds:

$$\mathsf{A} = (\mathsf{M}\mathsf{V})\mathsf{\Lambda}(\mathsf{M}\mathsf{V})^\mathsf{T}. \tag{6.8}$$

Using the matrices M, V, and $\mathsf{\Lambda}$, we define the operator $\mathsf{H} : \mathbb{R} \to \mathbb{R}^{n_\Lambda \times n_\Lambda}$ as

$$\mathsf{H}(s) = (\mathsf{M}\mathsf{V})\mathsf{\Lambda}^\mathsf{s}(\mathsf{M}\mathsf{V})^\mathsf{T}. \tag{6.9}$$

An advantage of this construction is that its inverse can be directly computed as $\mathsf{H}(s)^{-1} = \mathsf{V}\mathsf{\Lambda}^{-s}\mathsf{V}^{\mathsf{T}}$ due to $\mathsf{V}^{\mathsf{T}}\mathsf{M}\mathsf{V} = \mathsf{I}$. Next, we emphasize that $\mathsf{H}(0) = \mathsf{M}$ and $\mathsf{H}(1) = \mathsf{A}$, *i.e.* the discrete $L^2(\Gamma)$ and $H^1(\Gamma)$ norms on Λ_h are generated for $s = 0$ and $s = 1$, respectively. As a generalization, the norm induced by the matrix $\mathsf{H}(s)$ is equivalent to the $H^s(\Gamma)$ norm on the discrete space Λ_h [22]. In other words,

$$\|\phi\|_{s,\Gamma}^2 \lesssim (\pi\phi)^T \mathsf{H}(s)(\pi\phi) \lesssim \|\phi\|_{s,\Gamma}^2, \tag{6.10}$$

in which π is the representation operator in the basis $\{\phi_i\}_{i=1}^{n_\Lambda}$.

Next, we use these tools to define our preconditioner following the strategy of [26]. The operator $\mathsf{P}^{-1} : \mathbb{R}^{n_\Lambda} \to \mathbb{R}^{n_\Lambda}$ is defined according to the norm $\|\cdot\|_\Lambda$ from (4.5):

$$\mathsf{P}^{-1} := \mu\mathsf{H}\left(\tfrac{1}{2}\right) + K^{-1}\mathsf{H}\left(-\tfrac{1}{2}\right). \tag{6.11}$$

Defining $\mathcal{P}^{-1} := \pi^T\mathsf{P}^{-1}\pi$, we obtain the equivalence relation (6.5) by construction. In turn, the inverse operator $\mathcal{P}$ is an optimal preconditioner for the system (6.1). The matrix P is explicitly computed using the properties of V and M:

$$\mathsf{P} = \left(\mu\mathsf{H}\left(\tfrac{1}{2}\right) + K^{-1}\mathsf{H}\left(-\tfrac{1}{2}\right)\right)^{-1} = \mathsf{V}\left(\mu\mathsf{\Lambda}^{\frac{1}{2}} + K^{-1}\mathsf{\Lambda}^{-\frac{1}{2}}\right)^{-1}\mathsf{V}^{\mathsf{T}}. \tag{6.12}$$

6.3. An iterative method respecting mass conservation

The Steklov–Poincaré system from Section 6.1 and the preconditioner from Section 6.2 form the main ingredients of the iterative scheme proposed next. As mentioned before, we aim to use a Krylov subspace method on the reduced system (6.1). We turn to the Generalized Minimal Residual (GMRes) method [35] and propose the scheme we refer to as Algorithm 1, described below.

Algorithm 1

1. Set the tolerance $\epsilon > 0$, choose an initial guess $\phi_h^0 \in \Lambda_h$, and construct the right-hand side χ_h from (6.4b) and P from (6.12).
2. Using P as a preconditioner, apply GMRes to the discrete Steklov–Poincaré system (6.1) until the relative, preconditioned residual is smaller than ϵ. This involves solving a Stokes and a Darcy subproblem in (6.4a) at each iteration.
3. Construct $(\boldsymbol{u}_{S,h}, p_{S,h}) \in \boldsymbol{V}_{S,h} \times W_{S,h}$ and $(\boldsymbol{u}_{D,h}, p_{D,h}) \in \boldsymbol{V}_{D,h} \times W_{D,h}$ by solving the independent Stokes and Darcy subproblems with ϕ_h as the normal flux on Γ.
4. In the case of Neumann problems, reconstruct the mean of the pressure in Ω_D using (4.22) or (4.28).

We make three observations concerning this algorithm. Most importantly, the solution $(\boldsymbol{u}_h, p_h)$ produced by Algorithm 1 conserves mass locally, independent of the number of GMRes iterations. In particular, the definition of the space $\boldsymbol{V}_h$ ensures that no mass is lost across the interface. Moreover, with the flux ϕ_h given on the interface, the reconstruction in step (3) ensures that mass is conserved in each subdomain.

Secondly, we emphasize that the solves for the Stokes and Darcy subproblems in step 2 can be performed in parallel by optimized solvers. Moreover, the preconditioner is local to the interface and is agnostic to the choice of extension operators and chosen discretization methods. In turn, this scheme is applicable to a wide range of well-established "legacy" codes tailored to solving Stokes and Darcy flow problems.

Third, we have made the implicit assumption that obtaining P by solving (6.7) is computationally feasible. This is typically the case if the dimension of the interface space Λ_h is sufficiently small. The generalized eigenvalue problem is solved once in an *a priori*, or "off-line", stage and the assembled matrix P is then applied in each iteration of the GMRes method.

7. Numerical results

In this section, we present numerical experiments that verify the theoretical results presented above. By setting up artificial coupled Stokes–Darcy problems in two dimension, we investigate the dependency of Algorithm 1 on physical and discretization parameters in Section 7.1. Afterward, Section 7.2 presents a comparison of the proposed scheme to a Neumann–Neumann method.

7.1. Parameter robustness

Let the subdomains be given by $\Omega_S := (0,1) \times (0,1)$, $\Omega_D := (0,1) \times (-1,0)$, and $\Gamma := [0,1] \times \{0\}$. Two test cases are considered, defined by different boundary conditions. The first concerns the setting in which both the Stokes and Darcy subproblems are well-posed. On the other hand, test case 2 illustrates the scenario in which a pure Neumann problem is imposed on the porous medium.

For test case 1, let $\partial_\sigma \Omega_S$ be the top boundary ($x_2 = 1$) and $\partial_u \Omega_D$ the bottom boundary ($x_2 = -1$). The remaining portions of the boundary $\partial\Omega$ form $\partial_u \Omega_S$ and $\partial_p \Omega_D$. On $\partial_u \Omega_S$, zero velocity is imposed as described by (2.1f). The pressure data is set to $g_p(x_1, x_2) := x_2$ on $\partial_p \Omega_D$ to stimulate a flow field that infiltrates the porous medium.

Test case 2 simulates parallel flow over a porous medium. We impose no-flux conditions on $\partial\Omega_D \setminus \Gamma$, thereby ensuring that all mass transfer to and from the porous medium occurs at the interface Γ. The flow is stimulated by prescribing the velocity at the left and right boundaries of Ω_S using the parabolic profile $\boldsymbol{u}_S(x_1, x_2) := [0, x_2(2 - x_2)]$. As in test case 1, the top boundary represents $\partial_\sigma \Omega_S$, at which a zero stress is prescribed.

Both test cases consider zero body force and mass source, *i.e.* $\boldsymbol{f}_S := 0$ and $f_D := 0$. Moreover, we set the parameter α in the Beavers–Joseph–Saffman condition to zero for simplicity.

The meshes $\Omega_{S,h}$ and $\Omega_{D,h}$ are chosen to be matching at Γ and we set Γ_h as the coinciding trace mesh. Following Section 5, we choose the Mixed Finite Element method in both subdomains, implemented with the use of FEniCS [25]. The spaces are given by a vector of quadratic Lagrange elements ($\boldsymbol{P}_2$) for the Stokes velocity $\boldsymbol{V}_{S,h}$ and lowest order Raviart–Thomas elements (RT_0) for the Darcy velocity $\boldsymbol{V}_{D,h}$. The pressure space W_h is given by piecewise constants (P_0). The interface space Λ_h is chosen to be the normal trace of $\boldsymbol{V}_{S,h}$ on Γ_h, and therefore consists of quadratic Lagrange elements.

For the sake of efficiency, the matrices V and $\mathsf{\Lambda}$ used in the preconditioner P are computed *a priori*. Moreover, we pre-compute the LU-decompositions of the Darcy and Stokes subproblems. These decompositions serve as surrogates for optimized "legacy" codes. The iterative solver is terminated when a relative residual of $\epsilon = 10^{-6}$ is reached, *i.e.* when the ratio of Euclidean norms of the preconditioned residual and the preconditioned right-hand side is smaller than ϵ.

We first consider the dependency of the iterative solver on the mesh size. We set unit viscosity and permeability and start with a coarse mesh with $h = 1/8$. The mesh is refined four times and at each refinement, the number of iterations in Algorithm 1 is reported. The results for both test cases are shown in Table 1.

The results show that the number of iterations is robust with respect to the mesh size. Moreover, the second and third columns indicate the reduction from a fully coupled problem of size n_{total} to a significantly smaller interface problem of size n_Λ. As shown in Section 4, this interface problem is symmetric and positive definite.

We investigate the robustness of Algorithm 1 with respect to physical parameters by varying both the (scalar) permeability κ and the viscosity μ over a range of eight orders of magnitude. The number of iterations is reported in Table 2.

It is apparent that the scheme is robust with respect to both parameters, reaching the desired tolerance within a maximum of eleven iterations for the two test cases. Minor deviations in the iteration numbers can be observed for low permeabilities. The scheme may require an extra iteration in that case due to the higher sensitivity of the Darcy subproblem on flux boundary data.

TABLE 1. The number of iterations necessary to reach the given tolerance with respect to the mesh size. The material parameters are given by $\kappa = \mu = 1$.

$1/h$	n_{total}	n_Λ	Case 1	Case 2
8	1042	15	8	6
16	4002	31	9	8
32	15 682	63	8	9
64	62 082	127	8	9
128	247 042	255	8	8

TABLE 2. Number of iterations necessary to reach the tolerance with respect to the physical parameters. For both cases, the mesh size is set to $h = 1/64$.

Case 1		$\log_{10}(\mu)$				
		-4	-2	0	2	4
$\log_{10}(\kappa)$	4	8	8	8	8	8
	2	8	8	8	8	8
	0	8	8	8	8	8
	-2	7	7	7	7	7
	-4	7	7	7	7	7

Case 2		$\log_{10}(\mu)$				
		-4	-2	0	2	4
$\log_{10}(\kappa)$	4	9	9	9	9	9
	2	9	9	9	9	9
	0	9	9	9	9	9
	-2	9	9	9	9	9
	-4	11	11	11	11	10

7.2. Comparison to a Neumann–Neumann method

In order to compare the performance of Algorithm 1 to more conventional domain decomposition methods, we consider the closely-related Neumann–Neumann method. This method, as remarked in Remark 3.1 of [13], solves the Steklov–Poincaré system (6.1) in the following, iterative manner. Given the current residual, we solve the Stokes and Darcy subproblems by interpreting this residual as a normal stress, respectively pressure, boundary condition. The computed fluxes normal to Γ then update ϕ through the following operator:

$$\mathcal{P}_{\text{NN}} := \Sigma_{S,h}^{-1} + \Sigma_{D,h}^{-1}, \tag{7.1}$$

with $\Sigma_{S,h} + \Sigma_{D,h} = \Sigma_h$ the decomposition in (6.4a).

Noting that $\mathcal{P}_{\text{NN}}$ is an approximation of Σ_h^{-1}, we define the Neumann–Neumann method by replacing the preconditioner P by $\mathcal{P}_{\text{NN}}$ in Algorithm 1. Moreover, we choose the same Krylov subspace method (GMRes) and stopping criterion, in order to make the comparison as fair as possible.

We consider the numerical experiment from [10, 13] posed on $\Omega := (0,1) \times (0,2)$ with $\Omega_S := (0,1) \times (1,2)$, $\Omega_D := (0,1) \times (0,1)$, and $\Gamma = (0,1) \times \{1\}$. The solution is given by $\boldsymbol{u}_S := \big[(x_2-1)^2,\ x_1(x_1-1)\big]$, $p_S = \mu(x_1 + x_2 - 1) + (3K)^{-1}$, and $p_D = (x_1(1-x_1)(x_2-1) + \frac{1}{3}x_2^3 - x_2^2 + x_2)K^{-1} + \mu x_1$. The boundary conditions are chosen to comply with this solution and we impose the pressure on $\partial\Omega_D \setminus \Gamma$, the normal stress on the top boundary, and the velocity on the remaining boundaries of Ω_S. Finally, the Beavers–Joseph–Saffman condition is replaced by a no-slip condition for the tangential Stokes velocity on Γ.

Using the same Mixed Finite Element discretization as in the previous section, we vary the material and discretization parameters and report the number of iterations necessary to reach a relative residual of $\epsilon = 10^{-6}$ to the preconditioned problem. The results are presented in Table 3.

We observe that the two methods behave opposite as the mesh size decreases. Whereas the Neumann–Neumann method requires more iterations for finer grids, the performance of our proposed scheme appears to improve, requiring only eight iterations in all cases on the finest levels.

In general, Algorithm 1 outperforms the Neumann–Neumann method in terms of robustness, with the only deviation occurring in the case of a low permeability and a coarse grid. The Neumann–Neumann method appears

TABLE 3. Iteration counts of the proposed scheme compared to a Neumann–Neumann method. The initial mesh has $h_0 = 1/7$ and each refinement is such that $h_{i+1} = h_i/2$.

$\log_{10}(\mu)$	$\log_{10}(K)$	Neumann–Neumann					Algorithm 1				
		h_0	h_1	h_2	h_3	h_4	h_0	h_1	h_2	h_3	h_4
0	0	3	3	3	3	3	8	8	8	8	8
	−1	5	5	5	5	5	8	8	8	8	8
	−2	7	7	8	8	8	7	7	7	8	8
−1	0	5	5	5	5	5	8	8	8	8	8
	−1	7	7	8	8	8	7	7	7	8	8
	−2	8	9	12	16	13	10	9	8	7	7
−2	0	7	7	8	8	8	7	7	7	8	8
	−1	8	9	12	16	13	10	9	8	7	7
	−2	14	9	18	25	29	13	14	12	8	7

more sensitive to both material and discretization parameters and only converges faster for material parameters close to unity.

In terms of computational cost, we emphasize that our proposed scheme requires an off-line computation to construct the preconditioner and contains a solve for the Stokes and Darcy subproblems at each iteration. On the other hand, the Neumann–Neumann method requires an additional solve for the subproblems in the preconditioner $\mathcal{P}_{\mathrm{NN}}$. These additional solves will likely become prohibitively expensive for finer grids, since each solve is more costly and more iterations become necessary. Thus, if the preconditioner P can be formed efficiently, then Algorithm 1 forms an attractive alternative for such problems.

Although these results do not allow for a thorough, quantitative comparison with the Robin–Robin methods presented in [13], we do make an important, qualitative observation. In particular, our proposed method does not require setting any acceleration parameters and its performance is a direct consequence of the constructed preconditioner. This is advantageous because finding the optimal values for such parameters can be a non-trivial task.

8. Conclusion

In this work, we proposed an iterative method for solving coupled Stokes–Darcy problems that retains local mass conservation at each iteration. By introducing the normal flux at the interface, the original problem is reduced to a smaller problem concerning only this variable. Through *a priori* analysis with the use of weighted norms, a preconditioner is formed to ensure that the scheme is robust with respect to physical and discretization parameters.

Future research will focus on four main ideas. First, we are interesting in investigating the application of this scheme on different discretization methods, including the pairing of a MPFA finite volume method with the MAC-scheme as in [36].

Secondly, we note that the use of non-matching grids forms another natural extension. In that case, we aim to investigate how such a mismatch affects the discretization error. However, such analysis heavily depends on the chosen discretization method and is therefore reserved as a topic for future investigation.

Third, the generalization of these ideas to non-linear problems forms another area of our interest. By considering the Navier–Stokes equations in the free-flow subdomain, for example, the reduction to an interface problem will inherit the non-linearity. An iterative method that solves this reduced problem may benefit from a similarly constructed preconditioner.

Finally, as remarked in Section 6.3, we are under the assumption that the generalized eigenvalue problem (6.7) can be solved efficiently. However, if the assembly of P is too costly, then more efficient, spectrally equivalent

preconditioners are required. A promising example may be to employ the recent work on multi-grid preconditioners for fractional diffusion problems [3].

To conclude, we have presented this iterative method in a basic setting so that it may form a foundation for a variety of research topics that we aim to pursue in future work.

Acknowledgements. The author expresses his gratitude to Prof. Rainer Helmig, Prof. Ivan Yotov, Dennis Gläser, and Kilian Weishaupt for valuable discussions on closely related topics. Moreover, the author thanks the Deutsche Forschungsgemeinschaft (DFG, German Research Foundation) for supporting this work by funding SFB 1313, Project Number 327154368.

References

[1] T. Arbogast, L.C. Cowsar, M.F. Wheeler and I. Yotov, Mixed finite element methods on nonmatching multiblock grids. *SIAM J. Numer. Anal.* **37** (2000) 1295–1315.

[2] M.G. Armentano and M.L. Stockdale, A unified mixed finite element approximations of the Stokes–Darcy coupled problem. *Comput. Math. App.* **77** (2019) 2568–2584.

[3] T. Bærland, M. Kuchta and K.-A. Mardal, Multigrid methods for discrete fractional Sobolev spaces. *SIAM J. Sci. Comput.* **41** (2019) A948–A972.

[4] C. Bernardi and G. Raugel, Analysis of some finite elements for the Stokes problem. *Math. Comput.* **44** (1985) 71–79.

[5] D. Boffi, F. Brezzi and M. Fortin, Mixed Finite Element Methods and Applications. Springer **44** (2013).

[6] W.M. Boon, J.M. Nordbotten and I. Yotov, Robust discretization of flow in fractured porous media. *SIAM J. Numer. Anal.* **56** (2018) 2203–2233.

[7] F. Brezzi, J. Douglas and L.D. Marini, Two families of mixed finite elements for second order elliptic problems. *Numer. Math.* **47** (1985) 217–235.

[8] Y. Cao, M. Gunzburger, X. He and X. Wang, Robin–Robin domain decomposition methods for the steady-state Stokes–Darcy system with the Beavers–Joseph interface condition. *Numer. Math.* **117** (2011) 601–629.

[9] M. Discacciati, *Domain decomposition methods for the coupling of surface and groundwater flows*. Ph.D. thesis (2004).

[10] M. Discacciati, Iterative methods for Stokes/Darcy coupling. In: Domain Decomposition Methods in Science and Engineering. Springer (2005) 563–570.

[11] M. Discacciati and L. Gerardo-Giorda, Optimized schwarz methods for the Stokes–Darcy coupling. *IMA J. Numer. Anal.* **38** (2018) 1959–1983.

[12] M. Discacciati and A. Quarteroni, Navier–Stokes/Darcy coupling: modeling, analysis, and numerical approximation. *Rev. Mat. Complut.* **22** (2009) 315–426.

[13] M. Discacciati, A. Quarteroni and A. Valli, Robin–Robin domain decomposition methods for the Stokes–Darcy coupling. *SIAM J. Numer. Anal.* **45** (2007) 1246–1268.

[14] L. Evans, Partial Differential Equations. *Graduate Studies in Mathematics*. American Mathematical Society (2010).

[15] T. Fetzer, C. Grüninger, B. Flemisch and R. Helmig, On the conditions for coupling free flow and porous-medium flow in a finite volume framework. In: *International Conference on Finite Volumes for Complex Applications*. Springer (2017) 347–356.

[16] J. Galvis and M. Sarkis, Balancing domain decomposition methods for mortar coupling Stokes–Darcy systems. In: Domain Decomposition Methods in Science And Engineering XVI. Springer (2007) 373–380.

[17] M.J. Gander and T. Vanzan, On the derivation of optimized transmission conditions for the Stokes–Darcy coupling. In: Domain Decomposition Methods in Science and Engineering XXV (2019).

[18] G.N. Gatica, S. Meddahi and R. Oyarzúa, A conforming mixed finite-element method for the coupling of fluid flow with porous media flow. *IMA J. Numer. Anal.* **29** (2009) 86–108.

[19] G. Gatica, R. Oyarzúa and F.-J. Sayas, Analysis of fully-mixed finite element methods for the Stokes–Darcy coupled problem. *Math. Comput.* **80** (2011) 1911–1948.

[20] O. Iliev and V. Laptev, On numerical simulation of flow through oil filters. *Comput. Visual. Sci.* **6** (2004) 139–146.

[21] T. Karper, K.-A. Mardal and R. Winther, Unified finite element discretizations of coupled Darcy–Stokes flow. *Numer. Methods Part. Differ. Equ.* **25** (2009) 311–326.

[22] M. Kuchta, M. Nordaas, J.C. Verschaeve, M. Mortensen and K.-A. Mardal, Preconditioners for saddle point systems with trace constraints coupling 2D and 1D domains. *SIAM J. Sci. Comput.* **38** (2016) B962–B987.

[23] W.J. Layton, F. Schieweck and I. Yotov, Coupling fluid flow with porous media flow. *SIAM J. Numer. Anal.* **40** (2002) 2195–2218.

[24] J.L. Lions and E. Magenes, Non-Homogeneous Boundary Value Problems and Applications. Springer Science & Business Media **1** (2012).

[25] A. Logg, K.-A. Mardal and G. Wells, Automated Solution of Differential Equations by the Finite Element Method: The FEniCS Book. Springer Science & Business Media **84** (2012).

[26] K.-A. Mardal and R. Winther, Preconditioning discretizations of systems of partial differential equations. *Numer. Linear Algebra App.* **18** (2011) 1–40.

[27] R. Masson, L. Trenty and Y. Zhang, Coupling compositional liquid gas Darcy and free gas flows at porous and free-flow domains interface. *J. Comput. Phys.* **321** (2016) 708–728.

[28] K. Mosthaf, K. Baber, B. Flemisch, R. Helmig, A. Leijnse, I. Rybak and B. Wohlmuth, A coupling concept for two-phase compositional porous-medium and single-phase compositional free flow. *Water Resour. Res.* **47** (2011).

[29] J.M. Nordbotten, W.M. Boon, A. Fumagalli and E. Keilegavlen. Unified approach to discretization of flow in fractured porous media. *Comput. Geosci.* **23** (2019) 225–237.

[30] A. Quarteroni, A. Valli and P. Valli, Domain Decomposition Methods for Partial Differential Equations. *Numerical Mathematics and Scientific Computation*. Clarendon Press (1999).

[31] P.-A. Raviart and J.-M. Thomas, A mixed finite element method for 2-nd order elliptic problems. In: Mathematical Aspects of Finite Element Methods. Springer (1977) 292–315.

[32] B. Rivière and I. Yotov, Locally conservative coupling of Stokes and Darcy flows. *SIAM J. Numer. Anal.* **42** (2005) 1959–1977.

[33] I. Rybak, *Mathematical modeling of coupled free flow and porous medium systems*. Habilitation, University of Stuttgart (2016).

[34] I. Rybak, J. Magiera, R. Helmig and C. Rohde, Multirate time integration for coupled saturated/unsaturated porous medium and free flow systems. *Comput. Geosci.* **19** (2015) 299–309.

[35] Y. Saad and M.H. Schultz, GMRES: a generalized minimal residual algorithm for solving nonsymmetric linear systems. *SIAM J. Sci. Stat. Comput.* **7** (1986) 856–869.

[36] M. Schneider, K. Weishaupt, D. Gläser, W.M. Boon and R. Helmig, Coupling staggered-grid and MPFA finite volume methods for free flow/porous-medium flow problems. *J. Comput. Phys.* **401** (2020) 109012.